Università degli Studi di Modena e Reggio Emilia

Facoltà di Medicina e Chirurgia

Corso di Laurea Magistrale in Medicina e Chirurgia

Dipartimento delle Malattie dell'Apparato Respiratorio

Direttore: Prof. Enrico Clini

Dynamic Intrinsic PEEP and Respiratory Muscle Redistribution During High-Flow Nasal Cannula in Acute Exacerbation of COPD: A Physiological Proof-of-Concept Study

Relatore

Prof. Roberto Tonelli

Tesi di laurea di:

Giovanni Velardo

Anno Accademico 2025/2026

ABSTRACT

Background

Dynamic intrinsic positive end-expiratory pressure (PEEPi) is a key determinant of inspiratory loading during exacerbation of chronic obstructive pulmonary disease (ECOPD), imposing a threshold load that must be overcome before inspiratory flow can be generated. However, the extent to which dynamic PEEPi is associated with respiratory muscle redistribution, inspiratory effort, and ventilatory efficiency remains poorly characterized.

Methods

In this prospective physiological proof-of-concept study, patients with ECOPD underwent a comprehensive assessment of respiratory mechanics, inspiratory effort, respiratory muscle activity, breathing pattern, dyspnea, and gas exchange at baseline and after 2 hours of HFNC delivered under standardized conditions. HFNC was delivered at 40 L/min, with FiO_2 titrated to target an SpO_2 of 92-94%. Physiological measurements included dynamic PEEPi, Pes, Pdi, Pdi sniff, Pnose, diaphragm and accessory muscle ultrasound indices, Vte, respiratory rate (RR) and Borg dyspnoea score.

Results

Seven patients with ECOPD underwent complete physiological assessment. Higher dynamic PEEPi was associated with a pattern of respiratory muscle redistribution, characterized by lower diaphragm thickening fraction ($\rho = -0.68$) and greater intercostal and sternocleidomastoid thickening fractions ($\rho = 0.59$ and 0.81, respectively). This was paralleled by greater inspiratory effort, reflected by larger Pes, Pdi, and tidal Pnose swings ($\rho = 0.57$, 0.71, and 0.88, respectively). Finally, higher dynamic PEEPi was associated with lower ventilatory efficiency, reflected by lower Vte and Vte/PBW ($\rho = -0.71$ and -0.64, respectively), together with higher RR and Borg dyspnoea score ($\rho = 0.75$ and 0.95, respectively). Across the T0–T1 assessment, physiological trajectories were heterogeneous, suggesting that baseline dynamic PEEPi may modulate the short-term physiological response to HFNC.

Conclusions

Dynamic PEEPi may identify an unfavourable neuro-mechanical phenotype in ECOPD, characterized by inspiratory threshold loading, respiratory muscle redistribution, increased inspiratory effort, and impaired ventilatory efficiency. These findings support a physiology-guided approach to respiratory support and highlight the need for individualized monitoring during HFNC.

TABLE OF CONTENTS

1. INTRODUCTION

1.1 Acute Exacerbation of COPD (AECOPD): Definition, Epidemiology, and pathophysiology

Chronic obstructive pulmonary disease (COPD) is a leading global health issue, and exacerbations are major contributors to its morbidity and mortality. An acute exacerbation of chronic obstructive pulmonary disease (AECOPD) is characterized by increased dyspnoea and/or cough and sputum that worsens in less than 14 days which may be accompanied by tachypnoea and/or tachycardia and is often associated with increased local and systemic inflammation caused by infection, pollution, or other insult to the airways [1,2].

In Italy, approximately 74.000 hospitalizations for COPD were reported in 2023, with an average hospitalization rate of 1.49‰ and with a 30-day mortality after exacerbation of 9.55% [3].

Severe AECOPD causing acute respiratory failure (ARF) often requires admission to an intensive care unit (ICU). The prevalence reported in the literature on ICU admission rates ranges from 2 to 19% for AECOPD requiring hospitalization, with an in-hospital mortality rate of 20–40% and a re-hospitalization rate for a new severe event being 18% of the AECOPD cases admitted to ICUs [4].

AECOPD involves complex interactions between airway inflammation, mechanical stress, and systemic responses.

Exacerbations fundamentally reflect acute worsening of expiratory flow limitation (EFL) and there is evidence for both increased airway inflammatory activity and worsening airway obstruction as plausible explanations. In fact, during AECOPD airways resistance is abruptly increased (due to bronchospasm, mucosal oedema, and sputum inspissation) and this worsens EFL. The time constant for lung emptying (given by the product of resistance and compliance) is therefore prolonged and end-expiratory lung volume (EELV) is dynamically increased. Furthermore, the early collapse of terminal airways with air entrapment causes an intrinsic positive end-expiratory pressure (PEEPi). For this reason, any acute increase in ventilation (such as occurs with anxiety or transient hypoxaemia) can lead to dynamic hyperinflation (DH) in flow limited patients. DH is defined as a condition where the expiratory time (Texp) is insufficient to allow complete deflation of the lungs to the resting lung volume (EELV or functional residual capacity, FRC) before the subsequent inspiration. As a result, during exacerbations, patients tend to adopt a rapid shallow breathing pattern, further reducing the time available for lung emptying, thus promoting greater DH in a vicious cycle. The resulting increase in EELV reduces inspiratory capacity, forcing respiratory muscles to work against higher lung volumes, leading to inefficiency and increased work of breathing [5].

To interrupt this escalation, therapy of exacerbations is based on pharmacological management, which generally involves bronchodilators, corticosteroids and antibiotics for most patients. Oxygen therapy, physiotherapy, mucolytics, and airway clearance devices may be beneficial in selected cases[1].

Noninvasive mechanical ventilation (NIV) is the gold standard for managing AECOPD associated with respiratory acidosis[6].

In this population, NIV has been shown to reduce mortality and the need for endotracheal intubation compared to standard medical therapy. However, NIV may fail in 5-40% of AECOPD patients for several reasons, and invasive mechanical ventilation (IMV) is instituted[7]. In the recent years, High-Flow Nasal Oxygen (HFNO) has been introduced in the clinical practice as an alternative to NIV for acute-on-chronic hypercapnic respiratory failure of mild to moderate severity degree of respiratory acidosis[8].

1.2 Acute Respiratory Failure Secondary to AECOPD: Pathophysiological basis

Despite the ability of patients with severe COPD to maintain normal gas exchange and a compensated acid-base balance during stable periods, acute decompensation in the setting of an exacerbation is relatively common. Acute respiratory failure in patients with AECOPD is characterized by worsening hypoxemia, often accompanied by varying degrees of carbon dioxide (CO_2) retention and acidemia.

The causes of hypoxemia in this context generally fall into four categories: ventilation-perfusion (V/Q) mismatch, alveolar hypoventilation, impaired diffusion and increased shunting [5].

In COPD patients, hypoxemia is primarily due to an exacerbated V/Q mismatch, often associated with an increase in dead space, resulting in a subsequent relative alveolar hypoventilation [9].

Moreover, increased airway resistance and respiratory muscle overload lead to inadequate minute ventilation. These mechanisms also contribute to elevate arterial CO_2 levels ($PaCO_2$).

To maintain adequate alveolar ventilation and prevent rises in $PaCO_2$, patients often rely on an elevated respiratory rate. While this compensatory mechanism helps to maintain CO2 levels within physiological limits during stable phases, it becomes insufficient during exacerbations. As ventilatory mechanics deteriorate, the organism fails to eliminate excess CO_2, resulting in respiratory acidosis.

The onset of hypercapnia (acute hypercapnic respiratory failure) during AECOPD is strongly associated with both short- and long-term mortality in this population [5].

In some patients the use of higher amounts of supplemental oxygen may result in worsened CO_2 retention. This phenomenon is primarily attributed to a worsening of the V/Q ratio (due to the loss of hypoxic vasoconstriction) and the Haldane effect (hyperoxygenation results in reduced CO_2 carrying capacity by haemoglobin and decreased bicarbonate formation). The reduction in respiratory drive secondary to the suppression of hypoxic stimulation plays a minor role [10].

The gold standard for managing severe exacerbations presenting with acute respiratory failure with acidosis is NIV in Pressure Support Ventilation (PSV) mode. NIV improves gas exchange during AECOPD, with an increase in PaO_2, a decrease in $PA–aO_2$ (alveolar-arterial O_2 gradient) and a reduction in $PaCO_2$. This approach improves the ventilatory pattern by increasing tidal volume and minute ventilation and

thus reducing respiratory rate. Simultaneously, it reduces the work of breathing by supporting the function of the respiratory muscles [11].

HFNO might have a role as an alternative to NIV in AECOPD because of its ability to reduce work of breathing and because it determines a wash out from CO_2 of the pharyngeal dead space [12].

1.3 Distribution of Respiratory Effort Among Respiratory Muscles in Patients with AECOPD

The respiratory musculature consists of the diaphragm, intercostal muscles, abdominal muscles, and others accessory muscles (notably the sternocleidomastoids).

During acute exacerbations, the maximal pressure that can be generated by the respiratory muscles is reduced, as is the muscle efficiency (ratio of mechanical work output to the total metabolic cost) for the inspiratory muscles, especially the diaphragm. Therefore, the accessory muscles of breathing are maximally recruited and significant alterations in thoraco-abdominal pathway of motion is often evident[13].

The Diaphragm

The diaphragm is the primary inspiratory muscle, anatomically dome-shaped and divided into two main regions: the central tendon and the peripheral muscular portion. The muscular portion is further subdivided into the crural segment, medially attached to the lumbar vertebrae (L2-L4) via associated ligaments, and the larger costal segment, which is laterally positioned and anchored to the inner surfaces of the lower six ribs. During spontaneous breathing, diaphragmatic contraction has several effects: The central portion descends, driven by contraction of the appositional muscle fibres, leading to a reduction in pleural pressure (generating the negative intrathoracic pressure required for lung inflation) and an increase in abdominal pressure. This causes anterior displacement of the abdominal wall.

The costal fibres elevate the lower ribs, resulting in anterior and outward chest wall movement. To sustain rhythmic, uninterrupted respiration, the diaphragm fibers exhibit remarkable resistance to fatigue. Inspiratory muscles recover from fatigue ten times faster than other skeletal muscles due to their small fiber size, which minimizes oxygen diffusion distances and reduces oxygen consumption [14].

It has been observed that COPD patients may have a higher rate of diaphragmatic dysfunction (DD) with respect to age- and sex-matched healthy control individuals.

In stable COPD, respiratory muscle function is compromised due to increased elastic and resistive loads, altered mechanics, and elevated ventilatory demands. Pulmonary hyperinflation significantly impairs the ability of respiratory muscles, particularly the diaphragm, to generate pressure and flow. This leads to increased neural respiratory drive and greater workload for inspiratory muscles to maintain gas exchange. Over time, these changes cause alterations in the thoracic cage and diaphragm morphology

to accommodate the increased lung volumes, along with functional adaptations of muscle fibres to preserve strength and enhance endurance [15].

During AECOPD, additional systemic inflammation, oxidative stress, impaired energy balance, alterations in the biochemical environment (hypercapnia, acidosis, hypoxia, depletion of metabolic substrates), corticosteroid administration, inactivity, and bed rest may act as synergic mechanisms leading to DH [13].

Acute DH further shortens the inspiratory muscles, especially the diaphragm. Because the muscle is shorter during contraction, it generates less force and, for the diaphragm, its ability to generate negative pleural pressure, is impaired.

Moreover, higher intrathoracic pressures are needed to maintain an adequate Vt, and PEEPi acts as an adjunctive load that the respiratory muscles must overcome before generating inspiratory flow. Accessory muscles (intercostal, abdominal, and neck muscles) are thus recruited to support ventilation[16].

In severe AECOPD associated with prolonged near maximal loading of the inspiratory muscles and alterations in the metabolic milieu (acute hypoxia, hypercapnia, and acidosis combined with compromised blood flow), fatigue is almost inevitable, and NIV is often required to manage this condition.

NIV failure is strongly associated with severe diaphragmatic dysfunction, which can even lead to muscle paralysis. Acting on a predisposing mechanical substrate (low lung elastance) that favours volume overload, DH appears to be the main physiological mechanism which determines extreme diaphragmatic weakness [17].

Ultrasound imaging is a valuable technique for assessing diaphragmatic anatomy and function, particularly its motion and thickness.

Diaphragmatic mobility is evaluated by imaging the hemidiaphragms via the anterior subcostal window during spontaneous and forced breathing. Diaphragmatic thickness (Tdi) is measured using a linear probe placed at the appositional zone between the 8th and 9th ribs along the anterior axillary line, both at the end of expiration (Tdi exp) and at the end of inspiration (Tdi insp), during spontaneous and forced breathing.

The thickening fraction (TF), a key functional indicator, is calculated as [18]:

$$TF = \frac{Tdi\ insp - Tdi\ exp}{Tdi\ exp}\ x\ 100$$

A reduced TF indicates impaired diaphragmatic function and ineffective respiration. This measurement is critical in managing critically ill patients and has multiple applications: diagnosing diaphragmatic dysfunction, assessing respiratory workload, identifying diaphragmatic atrophy, and predicting outcomes for weaning from mechanical ventilation. In AECOPD requiring NIV, a Tdi < 20% during

spontaneous breathing is strongly associated with poor outcomes, including NIV failure, prolonged ICU stays, need for intubation and mechanical ventilation, longer ICU stays, as well as higher ICU, in-hospital, and 90-day overall mortality rates [19, 20].

The intercostal muscles

The intercostal muscles are composed of three thin layers of muscle fibres that occupy the intercostal spaces. The external intercostal muscles extend from the costal tubercles dorsally to the costochondral junctions, with fibres oriented obliquely downward and forward, from the upper rib to the lower rib. In the portion between the sternum and the costochondral junctions, the fibres are particularly thick in the parasternal region of the thoracic cage, where they are conventionally referred to as parasternal intercostals. These anatomical structures are active during the inspiratory phase and interact with the diaphragm and other inspiratory muscles.

In contrast, the internal intercostal muscles run obliquely upward and forward from the superior border of the lower rib to the inferior border of the upper rib and are traversed by nerves and blood vessels. The internal intercostals are active during the expiratory phase of the respiratory cycle. Studies examining the complex interaction of these muscles have shown that the dorsal third of the internal intercostals is active during the early phase of inspiration. In general, when the external intercostal muscles contract, their action on the lower rib is more pronounced than on the upper rib, while the internal intercostals exert their effects predominantly on the lower ribs [21].

The intercostal muscles can be evaluated using ultrasonography, with the parasternal region being the optimal site for assessment (specifically between the second and third ribs).

In healthy subjects the intercostal muscle thickness showed significant increases in the intercostal spaces of the anterior portion only during maximal breathing [22].

Intercostal muscle thickness is measured during ultrasound by identifying the hyperechoic borders of the muscle bundle, while functionality is assessed using the ratio of thickness during inspiration to thickness during expiration (intercostal thickening fraction, Tic) [23].

Twenty stable COPD patients underwent ultrasound measurement of thickness of parasternal intercostal muscles in relation to respiratory function tests. Lower intercostal muscle quantity and quality reflected greater COPD spirometric severity [24].

The clinical application of intercostal muscle ultrasonography is currently focused on weaning patients from IMV. Umbrello et al. observed twenty-one critically ill patients during pressure support ventilation and found a complex relationship between Tic and Tdi: a low Tdi could be associated with low or elevated levels of Tic. On the other hand, high levels of Tic were only present in the case of a low Tdi, suggesting that intercostal muscles may be recruited in case of an increased respiratory workload in the presence of diaphragm dysfunction [25].

Based on this evidence, ultrasound of the intercostal muscles is used in intensive settings during weaning from IMV. Activation of the diaphragm together with thickening of the intercostal muscles suggests effective spontaneous breathing, favouring successful weaning; the presence of diaphragmatic dysfunction combined with hyperactivation of the intercostal muscles is a negative prognostic indicator predicting weaning failure [26].

To date, no studies have evaluated the activity of intercostal muscles in spontaneously breathing patients with acute respiratory failure.

The sternocleidomastoid

The sternocleidomastoid (SCM) is a neck muscle that originates from two heads: one from the sternum and the other from the clavicle. The sternal head originates from the manubrium of the sternum, while the clavicular head arises from the superior surface of the clavicle. These two heads merge into a single belly that inserts into the mastoid process of the temporal bone of the skull.

The sternocleidomastoid has various functions: when activated unilaterally, it rotates the head to the opposite side, inclines it to the same side, and extends the head. When activated bilaterally, it flexes the neck if the thorax is the fixed point or elevates the thorax if the head is the fixed point. In the latter scenario, the sternocleidomastoid acts as an inspiratory muscle [14].

In stable COPD patients, during spontaneous breathing, the SCM remains electrically silent, with a high activation threshold, and is only activated when increased ventilation is required (e.g., during exercise or respiratory distress) [27, 28].

The reliability of ultrasonography for assessing changes in muscle thickness has been confirmed. Shiraishi et al. evaluated for the first time the association between ultrasound-calculated SCM thickening fraction (Tscm) and exercise tolerance in patients with COPD compared to healthy individuals. At rest, the SCM in COPD patients was thinner and showed a higher TF from end-expiration to resting inspiration than in controls, reflecting the increased respiratory effort required by these patients [29].

However, no studies have yet measured the Tscm via ultrasound in the acute setting in patients with respiratory failure.

1.4 Use of the esophageal pressure, nasal pressure and diaphragm pressure to assess the respiratory effort

Among the available monitoring tools, the ROX index and HACOR score have demonstrated high accuracy in predicting failure of HFNO and non-invasive ventilation (NIV) in patients with AHRF [30]. However, these indices do not consider respiratory effort, which plays a crucial role in the pathogenesis of pulmunary self induced lung injury (P-SILI) [31]. This limitation could be significant, as while HFNO has

been effective in improving oxygenation in hypoxic patients, it has proven to be insufficient in adequately reducing elevated respiratory efforts, especially when compared to NIV [32].

Currently, the gold standard for assessing respiratory effort is specific manometry, which measures the esophageal pressure swing (ΔPes) during the patient's breathing [33]. Prior studies have shown that the lack of reduction in ΔPes within the first two hours of NIV predicts failure of RS and the subsequent outcome (i.e. need for intubation) [34]. Despite its diagnostic utility, esophageal manometry has not been widely adopted in clinical practice due to several limitations, including invasiveness, cost, and a specialized training to warrant accurate interpretation [35]. As a result, its use has largely been confined to research settings.

Esophageal pressure

Esophageal pressure (Pes) is widely used as a surrogate measure of pleural pressure (Ppl) in both physiological and clinical studies of respiratory mechanics [36,38]. Because the esophagus is located within the thoracic cavity and is exposed to the surrounding intrathoracic pressure, the pressure measured by an esophageal balloon catheter closely reflects changes in pleural pressure, particularly in the middle and lower thirds of the esophagus [36,37]. Although absolute values of Pes may differ slightly from the true pleural pressure due to mediastinal weight, esophageal wall elastance, and regional variations in pleural pressure distribution, changes in Pes during spontaneous breathing are generally considered a reliable estimate of changes in pleural pressure [37,39].

The relationship between esophageal and pleural pressure is of particular importance for the assessment of transpulmonary pressure (PL), defined as the difference between alveolar pressure (Palv) and pleural pressure (PL = Palv – Ppl) [40,41]. Under static conditions (end-inspiration/end-expiration holds), Palv approximates airway pressure (Paw), while Ppl is estimated by Pes because the esophagus lies within the thorax, so that PL = Paw – Pes [40,41]

Since direct measurement of pleural pressure is invasive and impractical in routine clinical settings, esophageal pressure serves as a valuable surrogate, allowing estimation of lung-distending pressure and providing insight into respiratory mechanics, inspiratory effort, and patient–ventilator interaction[38,40].

During spontaneous inspiration, contraction of the diaphragm and inspiratory muscles generates a decrease in pleural pressure. This decrease is transmitted to the esophagus, resulting in a negative deflection of esophageal pressure [36,47]. Simultaneously, the negative intrathoracic pressure is transmitted to the upper airways, producing a reduction in nasal pressure. Consequently, fluctuations in nasal pressure during breathing are closely related to fluctuations in esophageal pressure, as both reflect the pressure generated by inspiratory muscle activity [42,44].

Nasal pressure

Nasal pressure (Pnas) represents a non-invasive surrogate signal of airflow and respiratory effort derived from pressure fluctuations measured at the nares using a nasal cannula connected to a pressure transducer [42,44]. Unlike flow sensors, which directly quantify volumetric airflow, nasal pressure reflects the pressure changes generated upstream of the upper airway during spontaneous breathing, providing an indirect but highly sensitive marker of inspiratory and expiratory dynamics[42,43]. From a physiological perspective, nasal pressure signals arise from the transmission of intrathoracic pressure swings generated by respiratory muscle activity to the upper airway opening. During spontaneous inspiration, diaphragmatic contraction reduces pleural pressure, generating a pressure gradient that propagates along the air column of the upper airway and results in a proportional drop in nasal pressure [42,44]. This relationship is particularly evident under conditions of stable upper airway patency, where airway resistance is low and pressure transmission is not significantly distorted by collapsibility or obstruction [42,43].

A key advantage of nasal pressure monitoring lies in its ability to detect subtle changes in inspiratory effort that may not be evident on thermistor-based airflow sensors. In sleep physiology, for example, nasal pressure is more sensitive in identifying flow limitation, hypopneas, and partial upper airway obstruction, as it preserves the contour of inspiratory flow limitation through flattening of the pressure waveform [43,44].

Importantly, nasal pressure variations show a temporal and qualitative correlation with esophageal pressure (Pes) swings, as both signals are ultimately driven by the same central respiratory motor output and inspiratory muscle activation [42,44]. In unobstructed conditions, a greater inspiratory effort is associated with a larger negative deflection in both Pes and Pnas, supporting the concept that nasal pressure can act as a downstream surrogate of respiratory drive. However, this relationship becomes progressively less linear in the presence of increased upper airway resistance, nasal obstruction, or dynamic airway collapse, where pressure dissipation and nonlinear flow dynamics distort the transmitted signal [43,44].

Several physiological and technical factors may influence the accuracy of nasal pressure as an estimator of respiratory effort. Mouth breathing can bypass nasal flow entirely, leading to signal attenuation or loss. Similarly, high levels of upper airway resistance may uncouple nasal pressure from true intrathoracic pressure swings, resulting in underestimation of inspiratory effort [43,44]. Dynamic pharyngeal collapse may further introduce nonlinearities in pressure transmission, limiting the quantitative interpretation of Pnas during obstructive events [43].

Despite these limitations, nasal pressure remains a clinically valuable tool due to its non-invasiveness, simplicity, and high temporal resolution. While it does not provide a direct quantitative estimate of pleural pressure comparable to esophageal manometry, it offers a robust surrogate for detecting

respiratory timing, inspiratory effort patterns, and airflow limitation, particularly in sleep medicine and in non-invasive respiratory monitoring contexts [42,44].

Diaphragmatic pressure

Diaphragmatic performance is classically quantified through transdiaphragmatic pressure (Pdi), defined as the pressure gradient across the diaphragm, calculated as the difference between abdominal and pleural pressure (Pdi = Pab − Ppl) [37,45]. In physiological and clinical practice, pleural pressure is commonly estimated by esophageal pressure (Pes), while abdominal pressure is approximated by gastric pressure (Pga), allowing Pdi to be expressed as Pdi = Pga − Pes [36,37] This index therefore represents the mechanical output generated specifically by diaphragmatic contraction and is considered the most direct surrogate of diaphragmatic strength and inspiratory muscle function [36,45].

During spontaneous inspiration, diaphragmatic contraction produces a caudal displacement of the abdominal contents, resulting in an increase in intra-abdominal pressure (Pga) and a simultaneous decrease in pleural pressure (Pes) [36,37]. The combined effect of these pressure changes generates a positive transdiaphragmatic pressure swing, which reflects the intensity of diaphragmatic activation and the effective pressure-generating capacity of the muscle [37,45]. In normal conditions, Pdi increases proportionally with inspiratory effort, making it a reliable physiological marker of respiratory muscle output.

Measurement of Pdi requires the simultaneous use of two intraluminal balloon catheters, one positioned in the esophagus and one in the stomach, enabling continuous recording of Pes and Pga [36,37]. Although technically more complex than isolated esophageal manometry, this approach remains the reference standard for direct assessment of diaphragmatic function in both experimental physiology and selected clinical settings [36,45].

Clinically, Pdi is used to evaluate diaphragmatic strength, detect dysfunction, and quantify inspiratory muscle load. Reduced Pdi values may indicate diaphragmatic weakness or paralysis, whereas excessive increases in Pdi may reflect increased respiratory drive and high work of breathing, as observed in acute respiratory failure or chronic obstructive pulmonary disease [38,45]. In the context of mechanical ventilation, Pdi provides important information regarding patient effort and patient–ventilator interaction, helping to identify both under-assistance and over-assistance conditions [38,46].

Given the invasive nature of Pdi measurement, surrogate indices such as esophageal pressure swings (ΔPes) and ultrasound-based diaphragmatic thickening fraction are frequently used in clinical practice to approximate inspiratory effort, although they do not fully replace direct Pdi measurement [45,46].

1.5 Respiratory Effort in Patients with Acute Respiratory Failure in spontaneous breathing

In recent years, non-invasive respiratory supports (NRS) are increasingly used as a first step in acute respiratory failure (ARF) treatment, despite protective IMV remains a cornerstone of the management of patients with severe hypoxemia [8].

An increasing body of evidence has demonstrated that precise monitoring of patients with ARF is crucial for the success of NIV treatment. NIV parameters must be adjusted according to the patient's clinical status and the severity of respiratory failure. These two factors are critical in determining the appropriate setting for administering NIV: inadequate care intensity can easily lead to NIV failure, delaying invasive ventilation and worsening patient outcomes [47].

In this scenario, monitoring and mitigating excessive respiratory effort in spontaneously breathing patients is becoming the key in the management of many ARF patients [48].

Esophageal manometry pressure (P_{es}) with swing (ΔP_{es}) assessment is considered the gold standard for the inspiratory effort evaluation during spontaneous breathing. It is measured using a nasogastric tube equipped with a pressure transducer to measure P_{es}.

P_{es} represents an accurate surrogate for pleural pressure (PPl) and coincides with the dynamic transpulmonary pressure during spontaneous breathing, providing a quantitative parameter of respiratory effort. Values over 10–12 cm H2O might be considered a threshold risk for patient self-inflicted lung injury (P-SILI) development, and its monitoring over time could be very useful in the early identification of NRS failure [49].

Changes in ΔP_{es} values within the first 2 hours of NIV initiation have been strongly correlated with ventilatory failure within 24 hours, with a threshold reduction in ΔP_{es} after the initiation of NIV of 10 cmH_2O [34].

However, esophageal manometry may be challenging to apply in patients with severe respiratory distress, requires substantial expertise, and is associated with high costs.

Nasal pressure swings (ΔP_{nose}) can be easily measured at the patient's bedside ad it is a physiological variable that reflects the airway pressure (Paw) swings captured in the upper respiratory tract during tidal breathing. ΔP_{nose} is strongly correlated with ΔP_{es}, and recent studies have shown it may play a role in predicting the failure of NRS [50].

1.6 PEEP, what is it and why is it important in COPD patients.

Positive end-expiratory pressure (PEEP) is a fundamental component of modern mechanical ventilation, defined as the pressure maintained in the airways at the end of expiration above atmospheric pressure [51,53]. Its primary physiological role is to prevent alveolar collapse at end-expiration, thereby increasing functional residual capacity (FRC), improving ventilation–perfusion matching, and reducing intrapulmonary shunt [52,53]. By maintaining a baseline distending pressure,

PEEP shifts the pressure–volume relationship of the respiratory system towards higher lung volumes and reduces the cyclic opening and closing of unstable alveolar units, a key mechanism of ventilator-induced lung injury (VILI) prevention [53,55].

From a physiological standpoint, PEEP can be conceptualized as either **external (set) PEEP** or **intrinsic (auto-PEEP)**. External PEEP is the pressure applied by the ventilator at end-expiration, whereas intrinsic PEEP (PEEPi) results from incomplete lung emptying before the next inspiratory cycle begins, leading to gas trapping and dynamic hyperinflation [52,54]. PEEPi is particularly relevant in obstructive lung diseases, where expiratory flow limitation prevents full exhalation within the allotted expiratory time[54,55].

A further distinction is made between **static PEEP** and **dynamic PEEP effects**. Static PEEP refers to the set end-expiratory pressure measured under no-flow conditions, typically assessed during an end-expiratory hold maneuver on the ventilator, reflecting the baseline alveolar pressure maintained by the ventilator [51,53]. Dynamic aspects of PEEP, in contrast, are related to time-dependent phenomena such as air trapping, expiratory flow limitation, and regional differences in lung emptying, which generate variable alveolar pressures throughout the expiration phase [54,56]. In patients with heterogeneous lung mechanics, such as acute respiratory distress syndrome (ARDS) or chronic obstructive pulmonary disease (COPD), dynamic PEEP effects may lead to significant regional overdistension or under-recruitment depending on local time constants [53,56].

In **COPD**, the clinical relevance of PEEP is particularly pronounced due to the presence of increased airway resistance and prolonged expiratory time constants. These factors promote incomplete lung emptying and the development of intrinsic PEEP (auto-PEEP), which increases end-expiratory lung volume and imposes an inspiratory threshold load on the respiratory muscles [54,55]. Before inspiratory flow can begin, the respiratory muscles must first generate a negative pleural pressure sufficient to counterbalance PEEPi, thereby increasing the total mechanical work of breathing and predisposing to respiratory muscle fatigue[59,60]. In this context, the diaphragm operates at a mechanical disadvantage: hyperinflation shortens its resting length, flattens its curvature, and reduces its force-generating capacity [61,62]. As diaphragmatic efficiency declines, compensatory recruitment of extra-diaphragmatic inspiratory muscles (i.e, the parasternal intercostals and the sternocleidomastoid) becomes necessary to sustain ventilation; however, this pattern has been associated with greater disease severity, higher dyspnea burden, and worse clinical outcomes [63,64].

In mechanically ventilated COPD patients, the application of external PEEP can be beneficial when carefully titrated, as it may counterbalance intrinsic PEEP, reduce inspiratory effort, and improve patient–ventilator synchrony [55,57]. However, excessive external PEEP may worsen hyperinflation and hemodynamic compromise by increasing intrathoracic pressure and reducing venous return [53,55].

Measurement of PEEP depends on the clinical context. In mechanically ventilated patients, PEEP is directly set on the ventilator and can be confirmed through an **end-expiratory occlusion (pause) maneuver**, which allows equilibration between alveolar pressure and airway opening pressure under zero-flow conditions [51,53]. Intrinsic PEEP is measured by performing an end-expiratory hold and assessing the pressure required to initiate inspiratory flow, often combined with esophageal pressure monitoring to better characterize total respiratory system load [54,56]. In spontaneous breathing patients, indirect assessment of PEEP-related effects may be performed using esophageal pressure, airflow signals, and flow–volume loop analysis, particularly to detect dynamic hyperinflation and expiratory flow limitation [54,56].

Physiologically, the effects of PEEP are closely linked to lung recruitability and chest wall mechanics. In recruitable lungs, moderate levels of PEEP improve oxygenation by reopening collapsed alveoli and stabilizing alveolar units, whereas in non-recruitable lungs, the same level of PEEP may primarily induce overdistension, increasing dead space ventilation and impairing hemodynamic [53,58]. The balance between recruitment and overdistension is therefore central to individualized PEEP titration strategies, particularly in ARDS management, where lung-protective ventilation strategies aim to optimize end-expiratory lung volume while minimizing driving pressure [53,58].

Overall, PEEP represents a key determinant of respiratory system mechanics, oxygenation, and patient–ventilator interaction. Its physiological effects depend on the interaction between applied pressure, intrinsic hyperinflation, and regional lung mechanics, making its optimal titration a cornerstone of both critical care ventilation and obstructive lung disease management [52,55].

1.7 Treatment of COPD

Non-invasive ventilation (NIV) remains the cornerstone of ventilatory support in ECOPD with acute hypercapnic respiratory failure, largely because the application of external end-expiratory pressure (PEEP) can counterbalance PEEPi, reduce the inspiratory threshold load, while pressure support unload the respiratory muscles and increase tidal volume. High-flow nasal cannula (HFNC) has emerged as an alternative or complementary modality, offering several physiological advantages including washout of upper airway dead space, improved ventilatory efficiency, generation of variable PEEP, and enhanced patient comfort and tolerance. In patients with COPD, HFNC has been shown to reduce the neuro-ventilatory drive, the work of breathing, and the respiratory rate (RR), while improving gas exchange. However, the level of external PEEP generated by HFNC may be insufficient to fully counterbalance PEEPi in patients with significant dynamic hyperinflation . Accordingly, the physiological response to HFNC in ECOPD is likely to be heterogeneous and critically dependent on the magnitude of the underlying inspiratory threshold load.

Non-Invasive Ventilation (NIV) in COPD

Non-invasive ventilation (NIV) represents the cornerstone of ventilatory support in acute exacerbations of chronic obstructive pulmonary disease (COPD), particularly in the presence of acute hypercapnic respiratory failure [7,66]. It is defined as the delivery of positive pressure ventilation without an invasive airway (endotracheal tube), typically through a facemask interface, allowing assistance of both inspiratory and expiratory phases of the respiratory cycle while preserving airway defense mechanisms[65,66].

From a physiological standpoint, the primary therapeutic effect of NIV in COPD is the reduction of alveolar hypoventilation through pressure support ventilation, which increases tidal volume and improves minute ventilation, thereby reducing $PaCO_2$ [7,66]. Inspiratory positive airway pressure (IPAP) assists the inspiratory muscles by unloading the diaphragm and accessory muscles, effectively decreasing the pressure-time product (PTP) and work of breathing [51,66]. Expiratory positive airway pressure (EPAP), analogous to external PEEP, is particularly relevant in COPD because it can counterbalance intrinsic PEEP (PEEPi), thereby reducing the inspiratory threshold load required to initiate inspiratory flow [51,56].

Dynamic hyperinflation is a central pathophysiological feature in COPD exacerbations and results from expiratory flow limitation and incomplete lung emptying. NIV directly addresses this mechanism by prolonging expiratory time, improving alveolar ventilation, and reducing end-expiratory lung volume in patients with severe air trapping [51,56]. By partially unloading the respiratory muscles and improving respiratory mechanics, NIV reduces diaphragmatic fatigue and restores a more efficient length–tension relationship of the inspiratory muscles [51,66].

Clinically, the use of NIV in COPD exacerbations with respiratory acidosis (typically pH < 7.35 with elevated $PaCO_2$) has been consistently associated with reduced intubation rates, decreased hospital mortality, and shorter hospital length of stay [7,66]. These benefits are most pronounced in patients with moderate-to-severe exacerbations who remain conscious, hemodynamically stable, and able to protect the airway [65,66].

Patient–ventilator interaction is a critical determinant of NIV success. Asynchrony, excessive leaks, and patient discomfort can impair efficacy and increase the work of breathing. Monitoring of respiratory effort using surrogate markers such as esophageal pressure (ΔPes) or clinical indices of accessory muscle use may help optimize pressure settings and improve synchrony between patient demand and ventilator assistance [38,51]. In COPD patients, careful titration of EPAP is essential to avoid either insufficient counteraction of PEEPi or excessive external PEEP, which may worsen hyperinflation and hemodynamic compromise [56].

Compared with high-flow nasal cannula (HFNC), NIV provides a more robust form of ventilatory assistance, capable of directly augmenting alveolar ventilation and correcting respiratory acidosis.

While HFNC may improve oxygenation and reduce work of breathing in mild-to-moderate respiratory distress, NIV remains the preferred modality in hypercapnic respiratory failure due to its superior ability to unload respiratory muscles and reduce CO_2 retention [38,66].

Overall, NIV is a targeted ventilatory strategy that directly modifies respiratory mechanics by combining inspiratory assistance and expiratory pressure support, addressing the core pathophysiological abnormalities of COPD exacerbations, including dynamic hyperinflation, increased work of breathing, and ventilatory failure [7,56].

High-Flow Nasal Cannula (HFNC) in COPD

High-flow nasal cannula (HFNC) therapy is a non-invasive oxygen delivery system capable of providing heated and humidified gas mixtures at flow rates up to 60 L/min with a precisely titratable fraction of inspired oxygen (FiO_2) [51,68]. Unlike conventional low-flow oxygen systems, HFNC generates a flow that can match or exceed the patient's inspiratory demand, thereby reducing room air entrainment and improving the stability of delivered FiO_2 [67,68]. This feature is particularly relevant in patients with chronic obstructive pulmonary disease (COPD), in whom ventilatory demand is often increased due to elevated work of breathing and ventilation–perfusion mismatch.

From a physiological perspective, HFNC exerts several mechanisms of action that may be beneficial in COPD. First, the high flow rates generate a low level of positive airway pressure, particularly during expiration, which can partially counteract intrinsic positive end-expiratory pressure (PEEPi) and reduce dynamic hyperinflation [68,70]. Although this effect is variable and generally lower than that achieved with non-invasive ventilation (NIV), it may still contribute to a reduction in inspiratory threshold load and improve patient comfort [69].

Second, HFNC reduces anatomical dead space by continuously flushing the nasopharyngeal cavity, thereby decreasing CO_2 rebreathing and improving alveolar ventilation efficiency [67,68]. This mechanism is particularly relevant in COPD, where increased physiological dead space is a major determinant of hypercapnia. By reducing dead space ventilation, HFNC may contribute to a modest decrease in arterial carbon dioxide levels and respiratory drive in selected patients [68,70].

Third, the conditioning of inspired gas (heating and humidification) improves mucociliary clearance and enhances secretion management, which is clinically relevant in COPD patients with chronic bronchitis phenotype and mucus hypersecretion [67]. Improved secretion clearance may reduce airway resistance and contribute to a more effective expiratory flow, indirectly mitigating air trapping.

In addition, HFNC reduces the work of breathing by decreasing inspiratory resistance and providing a more consistent inspiratory flow pattern compared to conventional oxygen therapy [68,70]. This reduction in respiratory effort is reflected in decreased diaphragmatic load and improved ventilatory efficiency, although the magnitude of this effect is generally less pronounced than that observed with NIV in acute hypercapnic exacerbations [69,71].

Clinically, HFNC has been studied in COPD patients with varying severity of respiratory failure, including those with acute exacerbations and post-extubation respiratory support. Evidence suggests that HFNC may improve oxygenation and patient comfort, and in selected cases may reduce escalation to non-invasive ventilation or invasive mechanical ventilation, although its role in managing significant hypercapnic acidosis remains limited compared to NIV [69,71]. Current physiological and clinical data therefore support HFNC as a valuable adjunct in mild-to-moderate respiratory failure and in patients who are intolerant to NIV interfaces [70,71].

Overall, HFNC represents a supportive respiratory therapy that combines oxygen delivery, dead space washout, and low-level positive airway pressure, offering physiological benefits that are particularly relevant in COPD patients with increased work of breathing and dynamic hyperinflation, albeit without fully replacing the ventilatory support provided by NIV [68,71].

Despite the growing clinical use of HFNC in this population, the relationship between PEEPi and the physiological response to HFNC has never been systematically explored. It remains unknown whether and to what extent the degree of dynamic hyperinflation modulates the effects of HFNC on inspiratory effort, respiratory muscle recruitment, breathing pattern, and dyspnea. Esophageal and transdiaphragmatic pressure monitoring provide the reference standard for quantifying inspiratory effort and PEEPi, while respiratory muscle ultrasound (US) offers a complementary, non-invasive assessment of diaphragmatic and extra-diaphragmatic muscle activity. Nasal pressure swings (Pnose) have recently been proposed as a non-invasive surrogate of Pes swings in spontaneously breathing patients with acute respiratory failure, further expanding the bedside monitoring toolkit.

The aim of this prospective physiological proof-of-concept study was to characterize the relationship between dynamic PEEPi and inspiratory effort, respiratory muscle recruitment, breathing pattern, and dyspnea in patients with ECOPD treated with HFNC. We hypothesized that higher levels of dynamic PEEPi would be associated with greater inspiratory effort, increased extra-diaphragmatic muscle recruitment, a more unfavourable breathing pattern, and more severe dyspnea during HFNC, and that these associations would also modulate the physiological changes observed over the first hours of treatment.

2. MATERIALS AND METHODS

2.1 Study design and population

This was a prospective physiological proof-of-concept study conducted in the Respiratory Intermediate Care Unit of the University Hospital of Modena, Italy, between July 1st, 2025, and May 1st, 2026. Consecutive adult patients admitted with ECOPD and deemed suitable for an initial HFNC trial according to the institutional protocol were screened. Patients were eligible if they had acute hypercapnic respiratory failure secondary to ECOPD, with arterial pH >7.25, preserved consciousness, no severe respiratory distress, no immediate indication for NIV or endotracheal intubation, and preserved spontaneous breathing. Patients requiring immediate ventilatory assistance because of severe acidosis (i.e. pH <7.25), altered mental status, or severe respiratory distress were not considered eligible for HFNC. Exclusion criteria included inability to cooperate with physiological measurements, intolerance to HFNC, pregnancy, neuromuscular disorders affecting respiratory muscles, interstitial lung disease, or known diaphragmatic dysfunction unrelated to COPD. All enrolled patients received standard medical treatment for ECOPD according to current international guidelines, including bronchodilators, corticosteroids, antibiotics when clinically indicated, and oxygen supplementation. The study was approved by the local Ethics Committee (protocol number 165/2024/SPER/AOUMO SIRER ID 7354), and written informed consent was obtained from all participants.

2.2 High flow nasal cannula setting

HFNC treatment was delivered using the AIRVO™ 2 system (Fisher & Paykel Healthcare, Auckland, New Zealand). Flow was set at 40 L/min, gas temperature at 37°C, and FiO_2 was titrated to maintain peripheral oxygen saturation between 92% and 94%.

Patients underwent a comprehensive physiological assessment at HFNC initiation (T0) and after 2 hours of treatment (T1). Measurements included inspiratory effort, respiratory mechanics, respiratory muscle ultrasound, breathing pattern, gas exchange, and dyspnea.

2.3 Study assessment procedures

2.3.1 Inspiratory effort

Esophageal pressure (Pes) and gastric pressure (Pga) were measured using a balloon catheter system (NutriVent®, SIDAM, Mirandola, Italy) inserted through the nares according to standard techniques and connected to a dedicated pressure monitoring system (OptiVent®, SIDAM, Mirandola, Italy). Correct positioning of the esophageal and gastric balloons was verified by visual inspection of cardiac artifacts on the Pes tracing, and by chest X-Ray confirming the position of the radiopaque markers. Throughout the manuscript, Pes and Pdi refer to inspiratory tidal swings in esophageal and transdiaphragmatic pressure, respectively. Pes was calculated as the difference between end-expiratory esophageal pressure and the nadir inspiratory esophageal pressure during tidal breathing. Pdi was calculated as

the inspiratory increase in transdiaphragmatic pressure, derived as Pga minus Pes, from end-expiration to peak inspiration within the same breath.

Diaphragmatic pressure-generating capacity was assessed using the sniff maneuver (Pdisniff), defined as the maximal transdiaphragmatic pressure generated during repeated maximal sniff efforts starting from functional residual capacity. Sniff maneuvers were repeated at least three times or until reproducibility was achieved, and the highest value was retained for analysis.

Nasal pressure (Pnose) was measured during tidal breathing using a soft self-expanding foam plug with an embedded cannula inserted into one nostril (that allocating NutriVent®) and connected to a pressure transducer, while the contralateral nostril remained open during HFNC delivery[50]. Pnose swings were calculated as the difference between end-expiratory nasal pressure and the nadir inspiratory nasal pressure. Throughout the manuscript, Pnose refers to the tidal nasal pressure swing. All tidal physiological variables were averaged over at least 3 stable, artifact-free breaths. Tracings affected by swallowing, coughing, or signal instability were excluded.

2.3.2 Respiratory mechanics

Dynamic intrinsic positive end-expiratory pressure (PEEPi,dyn) and expiratory tidal volume (Vte) were assessed at T0 and T1 during a brief standardized interruption of HFNC. Airflow was measured using a flanged mouthpiece connected to a dedicated flow sensor integrated within the OptiVent® system (SIDAM, Mirandola, Italy), while a nose clip was applied during recordings. Airflow, Pes, and Pga signals were recorded simultaneously at a sampling rate of 200 Hz. HFNC was briefly interrupted, and recording was started immediately after removal of the nasal cannulae, without a washout period, to minimize dissipation of the physiological conditions present during HFNC. The total interruption time did not exceed 3 minutes, and HFNC was resumed immediately after acquisition.

PEEPi,dyn was defined as the negative deflection in Pes occurring between the onset of inspiratory effort and the zero-flow point, corresponding to the onset of inspiratory flow. The onset of inspiratory effort was identified from the Pes tracing as the point at which Pes began its negative deflection from the end-expiratory value. Because expiratory muscle activity may contribute to Pes deflection thus overestimating the true inspiratory threshold load, PEEPi,dyn was corrected for abdominal muscle contribution using the Pga total decay method. Pga total decay was defined as the fall in Pga from its end-expiratory value to its nadir during inspiration. Corrected PEEPi,dyn was calculated as uncorrected PEEPi,dyn minus Pga total decay and was used for all analyses.

Vte was calculated by digital integration of the expiratory flow signal and expressed both as absolute volume and normalized to predicted body weight (PBW).

All physiological variables were averaged over at least 3 stable, artifact-free breaths. Tracings affected by swallowing, coughing, or signal instability were excluded.

2.3.3 Respiratory muscle ultrasound

US assessment of inspiratory muscles was performed by a single experienced operator. The diaphragm was assessed at the zone of apposition of the right hemidiaphragm using a high-frequency linear probe. Diaphragm thickness was measured at end-expiration and end-inspiration, and diaphragm thickening fraction (TFdi) was calculated as:

$$TFdi = \frac{Tdi,insp - Tdi,exp}{Tdi,exp} \; x\; 100$$

Maximal diaphragmatic recruitment was additionally assessed during a maximal sniff maneuver. The diaphragmatic recruitment index (TMaxdi) was calculated as the ratio between diaphragm thickness at end-inspiration during tidal breathing and diaphragm thickness at end-inspiration during maximal sniff effort, as previously described.

$$TMaxdi = \frac{Tdi,insp,tidal}{Tdi,insp,sniff}$$

Parasternal intercostal and sternocleidomastoid muscles were assessed using standardized B-mode and M-mode approaches. Thickening fractions of intercostal (TFic) and sternocleidomastoid muscles (TFscm) were calculated using the same formula. Measurements were averaged over 3 consecutive respiratory cycles obtained during stable tidal breathing.

2.3.4 Clinical assessment

Respiratory rate (RR) was measured from airflow tracings during physiological recordings. Dyspnea was assessed using the modified Borg scale. Blood gas analysis was also recorded at T0 and T1.

2.4 Outcomes

The primary outcome of the study was the relationship between PEEPi,dyn and inspiratory effort, respiratory muscle recruitment, and breathing pattern during HFNC treatment in patients with ECOPD. Secondary outcomes included the relationship between PEEPi,dyn and changes in inspiratory effort, respiratory muscle recruitment, breathing pattern and gas exchange between T0 and T1.

2.5 Statistical analysis

Given the exploratory physiological nature of the study, no formal sample size calculation was performed. Continuous variables are reported as median and interquartile range (IQR). Correlations between baseline dynamic PEEPi and physiological variables were assessed using Spearman correlation analysis. Associations between dynamic PEEPi and changes in inspiratory effort, respiratory muscle activity, breathing pattern, and dyspnea during HFNC were similarly explored using Spearman correlation coefficients. All analyses were performed using GraphPad Prism (GraphPad Software, San Diego, CA, USA) and IBM SPSS Statistics (IBM Corp., Armonk, NY, USA).

3. RESULTS

3.1 Patient population

Seven patients with acute hypercapnic respiratory failure secondary to ECOPD underwent complete physiological assessment at HFNC initiation and after 2 hours of treatment. Individual clinical and gas-exchange data are reported in **Table 1**, while individual physiological measurements are reported in **Table 2**. Four patients were on single-inhaler triple therapy and three on dual LAMA/LABA therapy; three had received systemic corticosteroids in the previous 6 months. Chronic heart failure and diabetes were present in four and five patients, respectively.

At baseline, all patients were fully conscious and hemodynamically stable. Gas exchange was consistent with mild-to-moderate acute hypercapnic respiratory failure, with a median pH of 7.28, $PaCO_2$ of 66 mmHg, and PaO_2/FiO_2 of 151 mmHg. At baseline, dynamic intrinsic PEEP was measurable in all patients, with a median PEEPi,dyn of 4.2 cmH_2O. Inspiratory effort showed interindividual variability, with median Pes, Pdi, and Pnose swings of 10.0 cmH_2O, 16.4 cmH_2O, and 3.6 cmH_2O, respectively. Respiratory muscle US showed heterogeneous values of diaphragmatic, intercostal, and sternocleidomastoid thickening fraction, with median TFdi, TFic, and TFscm of 0.27, 0.05, and 0.06, respectively. Median Vte was 323 mL, RR was 25 breaths/min, and Borg dyspnea score was 5. After 2 hours of HFNC, gas exchange remained broadly stable, with a median pH of 7.28, $PaCO_2$ of 68 mmHg, and PaO_2/FiO_2 of 154 mmHg. Median PEEPi,dyn was 4.0 cmH_2O, Pes and Pnose swings were 9.0 cmH_2O and 3.2 cmH_2O, respectively, while Vte increased to 388 mL. RR decreased to 23 breaths/min and Borg dyspnea score to 3.

Figure 1. Study flowchart.

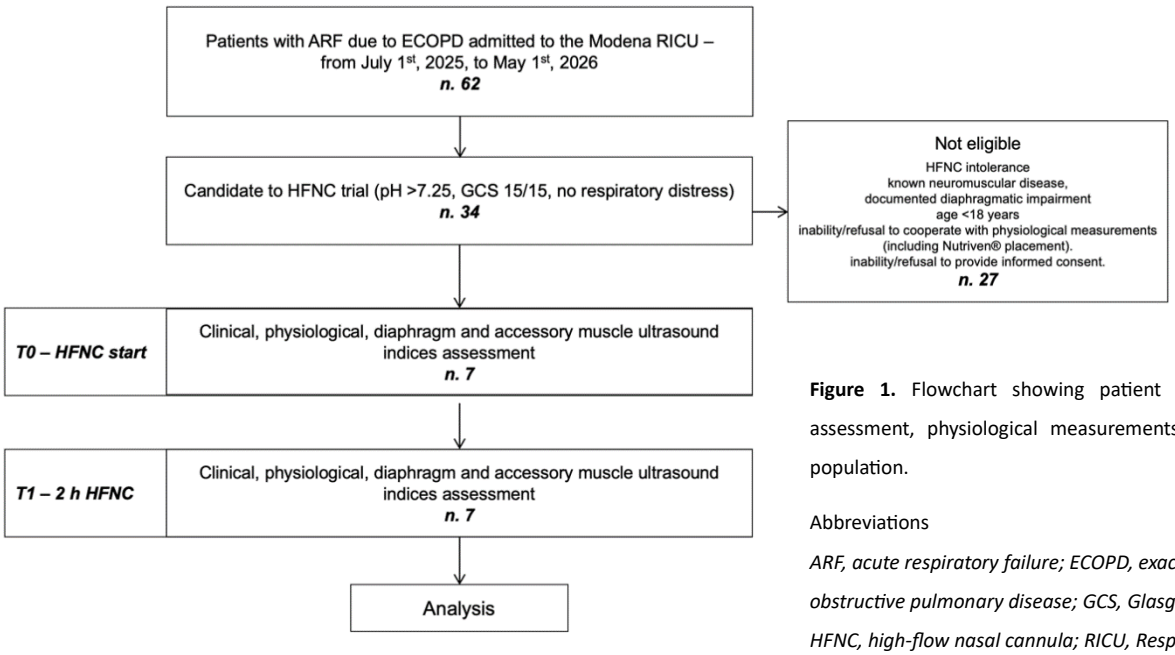

Figure 1. Flowchart showing patient screening, eligibility assessment, physiological measurements, and final analysis population.

Abbreviations

ARF, acute respiratory failure; ECOPD, exacerbation of chronic obstructive pulmonary disease; GCS, Glasgow Coma Scale; HFNC, high-flow nasal cannula; RICU, Respiratory Intermediate Care Unit.

Table 1. Individual clinical and gas-exchange characteristics at T0 and T1

T0 – Baseline

N	GCS, value	MAP, mmHg	HR, bpm	pH	PaO_2/FiO_2, mmHg	PaO_2, mmHg	$PaCO_2$, mmHg	HCO_3-, mmol/L	BE, mmol/L	Lac, mmol/L
1	15	80	87	7.28	135	74,4	61.6	28.2	2.3	0.60
2	15	83	65	7.25	151	60,2	69.6	29.1	3.2	1.00
3	15	123	95	7.29	259	72,6	54.1	25.4	0.6	1.20
4	15	97	87	7.28	79	55,0	66.2	30.3	4.0	2.10
5	15	84	73	7.34	130	52,1	69.6	36.6	10.5	1.00
6	15	110	100	7.31	195	68,3	56.1	27.0	1.2	0.30
7	15	83	89	7.25	158	63,0	77.5	32.9	5.8	1.00
Median, IQR	15 (15-15)	84 (83-103)	87 (80-92)	7.28 (7.27-7.3)	151 (133-176)	63 (58-70)	66 (59-70)	29.1 (28-31.6)	3.2 (1.8-4.9)	1 (0.8-1.1)

T1 – 2 hours after HFNC

N	GCS, value	MAP, mmHg	HR, bpm	pH	PaO_2/FiO_2, mmHg	PaO_2, mmHg	$PaCO_2$, mmHg	HCO_3-, mmol/L	BE, mmol/L	Lac, mmol/L
1	15	93	87	7.24	120	72.0	64.2	26.5	-0,2	1,40
2	15	113	68	7.21	116	58.0	76.1	29.4	2,0	2,60
3	15	124	97	7.34	217	62.0	50.2	27.1	1,7	0,90
4	15	90	85	7.24	154	54.0	72.3	29.8	2,8	2,40
5	15	113	68	7.35	145	58.0	67.5	36.2	9,8	0,90
6	15	103	100	7.36	217	65.0	48.1	26,2	1,1	0,40
7	15	**93**	92	7.27	232	62.0	69.4	30.8	6,6	1,00
Median, IQR	15 (15-15)	103 (93-113)	87 (87-95)	7.28 (7.24-7.35)	154 (133-217)	72 (58-82)	68 (57-71)	29.4 (26.3-32)	2 (1.4-4.7)	1 (0.9-1)

Table 1. Individual clinical and arterial blood gas variables are reported for each patient at T0, corresponding to baseline assessment at HFNC initiation, and at T1, corresponding to reassessment after 2 hours of HFNC treatment. Summary data are reported as median and interquartile range.

Abbreviations

BE, base excess; GCS, Glasgow Coma Scale; HCO_3^-, bicarbonate; HFNC, high-flow nasal cannula; HR, heart rate; IQR, interquartile range; Lac, lactate; MAP, mean arterial pressure; $PaCO_2$, arterial partial pressure of carbon dioxide; PaO_2, arterial partial pressure of oxygen; PaO_2/FiO_2, ratio of arterial oxygen partial pressure to inspired oxygen fraction.

Table 2. Individual physiological characteristics at HFNC initiation and after 2 hours of treatment.

T0 – Baseline

N	PEEPi, dyn, cmH_2O	Pes, cmH_2O	Pdi, cmH_2O	Pnose, cmH_2O	Pdisniff, cmH_2O	TFdi, ratio	TFi, ratio	TFscm, ratio	TMaxdi, ratio	Vte, mL	Vte/PBW, mL/kg	RR, bpm	Borg, score
1	8.7	18.2	26.2	8.7	31.3	0.15	0.30	0.11	0.88	180	3.7	32	7
2	7.3	20.8	19.4	9.2	21.3	0.17	0.40	0.19	0.91	167	2.8	28	6
3	4.2	7.5	14.4	3.6	81.2	0.41	0.00	0.05	0.66	385	5.8	22	5
4	5.9	19.9	23.6	8.9	26.4	0.14	0.80	0.35	1.00	202	3.3	29	6
5	4.1	8.6	13.5	3.6	77.2	0.27	0.00	0.06	0.83	354	6.1	25	3
6	3.4	10.2	14.3	2.6	89.2	0.29	0.00	0.00	0.62	403	5.9	24	4
7	3.2	9.8	16.4	2.0	77.2	0.38	0.05	0.00	0.63	323	4.4	23	2
Median, IQR	4.2 (3.8-6.6)	10 (9.2-19)	16.4 (14.4-21.5)	3.6 (3.1-8.8)	77.2 (28.9-79.2)	0.27 (0.16-0.33)	0.05 (0-0.35)	0.06 (0.03-0.15)	0.83 (0.64-0.9)	323 (191-370)	4.4 (3.5-5.9)	25 (23.5-28.5)	5 (3.5-6)

T1 – 2 hours after HFNC

N	PEEPi, dyn, cmH_2O	Pes, cmH_2O	Pdi, cmH_2O	Pnose, cmH_2O	Pdisniff, cmH_2O	TFdi, ratio	TFic, ratio	TFscm, ratio	TMaxdi, ratio	Vte, mL	Vte/PBW, mL/kg	RR, bpm	Borg, score
1	8.5	18.7	24.0	9.4	28.0	0.10	0.39	0.18	0.88	174	3.6	29	6
2	8.1	23.2	17.8	10.5	21.0	0.11	0.70	0.25	0.95	155	2.6	26	6
3	4.0	6.5	16.0	2.8	81.0	0.41	0.00	0.00	0.66	395	6.0	23	3
4	6.5	21.2	20.0	10.2	24.0	0.14	0.90	0.45	1.00	186	3.0	26	6
5	3.2	8.0	17.0	3.2	81.0	0.33	0.00	0.06	0.70	388	6.7	16	3
6	2.1	7.2	12.0	1.8	89.0	0.39	0.00	0.00	0.60	433	6.4	20	3
7	2.2	9.0	21.2	1.8	92.0	0.44	0.00	0.00	0.59	402	5.5	18	2
Median, IQR	4 (2.7-7.3)	9 (7.6-20)	17.8 (16.5-20.6)	3.2 (2.3-9.8)	81.2 (26.3-85.3)	0.33 (0.13-0.4)	0 (0-0.55)	0.06 (0-0.22)	0.7 (0.63-0.92)	388 (180-399)	5.5 (3.3-6.2)	23 (19-26)	3 (3-6)

Table 2. Individual respiratory mechanics, inspiratory effort, respiratory muscle ultrasound, breathing pattern, and dyspnea variables are reported for each patient at T0, corresponding to baseline assessment at HFNC initiation, and at T1, corresponding to reassessment after 2 hours of HFNC treatment. Summary data are reported as median and interquartile range.

Abbreviations

HFNC, high-flow nasal cannula; IQR, interquartile range; PBW, predicted body weight; Pdi, transdiaphragmatic pressure swing; Pdi,sniff, maximal transdiaphragmatic pressure during sniff maneuver; PEEPi,dyn, dynamic intrinsic positive end-expiratory pressure; Pes, esophageal pressure swing; Pnose, tidal nasal pressure swing; RR, respiratory rate; TFdi, diaphragmatic thickening fraction; TFic, intercostal thickening fraction; TFscm, sternocleidomastoid thickening fraction; TMaxdi, tidal-to-maximal diaphragmatic thickening ratio; Vte, expiratory tidal volume; Vte/PBW, expiratory tidal volume normalized to predicted body weight.

3.2 Dynamic PEEPi and baseline physiological variables

Figure 2 shows the association between dynamic PEEPi and inspiratory effort. Direct correlation was observed for tidal Pes (ρ=0.57, **panel A**), Pdi (ρ=0.71, **panel B**), and Pnose (ρ=0.88, **panel D**), while Pdisniff showed an inverse correlation (ρ=−0.68, **panel C**). Respiratory muscle US indices are presented in **Figure 3**. Dynamic PEEPi was inversely correlated with TFdi (ρ=−0.68, **panel A**) and directly correlated with TFic (ρ=0.59, **panel B**), TFscm (ρ=0.81, **panel C**), and TMaxdi (ρ=0.79, **panel D**). **Figure 4** reports the associations with breathing pattern and dyspnea. Dynamic PEEPi was inversely correlated with Vte and Vte/PBW (ρ=−0.71 and ρ=−0.64, **panel A** and **B**, respectively), whereas direct correlations were observed with Borg dyspnea score and RR (ρ=0.95 and ρ=0.75, **panel C** and **D**, respectively).

Figure 2. Association between dynamic intrinsic PEEP and inspiratory effort.

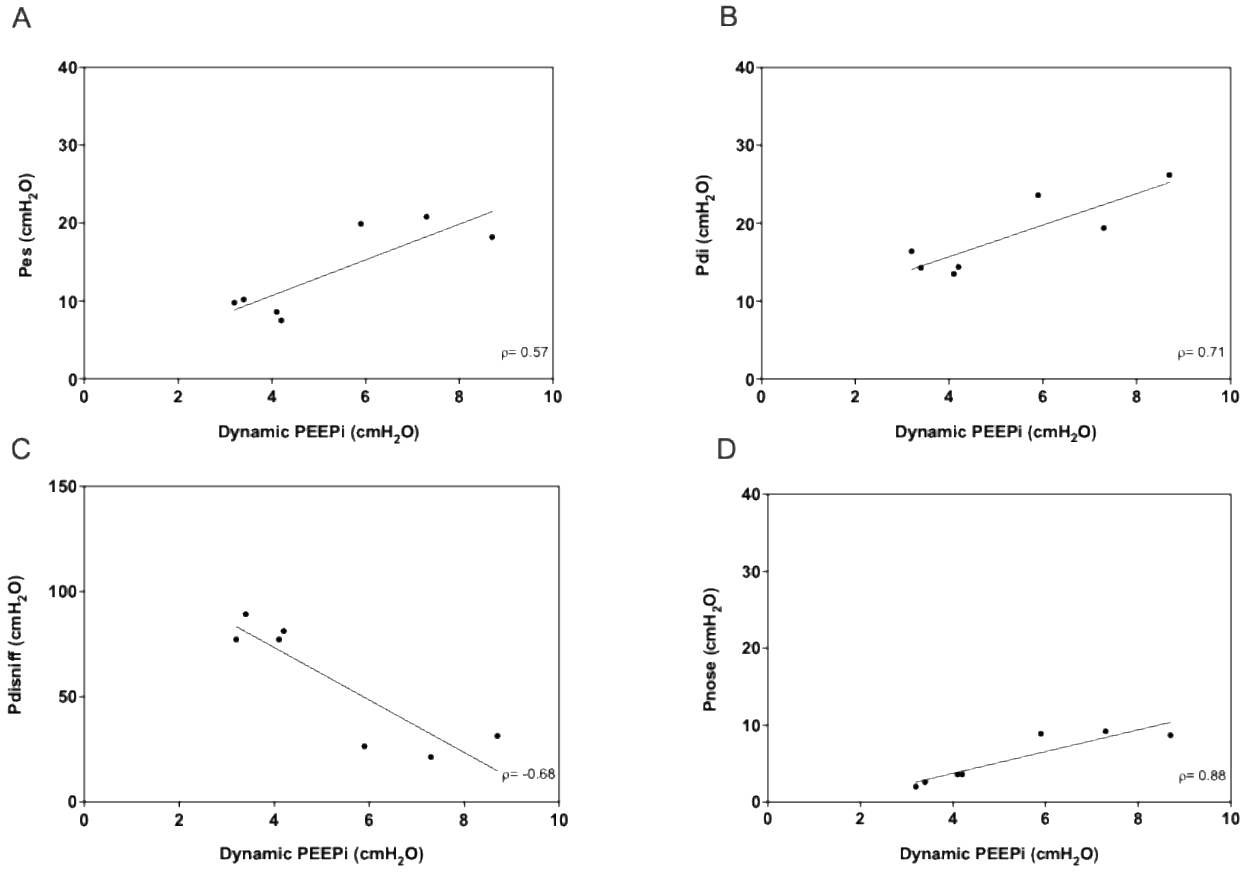

Figure 2. Scatterplots showing the relationship between dynamic intrinsic positive end-expiratory pressure (PEEPi,dyn) and indices of inspiratory effort in patients with ECOPD treated with HFNC. Dynamic PEEPi was directly correlated with tidal esophageal pressure swing (Pes; A), transdiaphragmatic pressure swing (Pdi; B), and tidal nasal pressure swing (Pnose; D), while an inverse correlation was observed with maximal transdiaphragmatic pressure during sniff maneuver (Pdi,sniff; C). Spearman correlation coefficients are reported in each panel. Lines represent linear fit for visual display.

Abbreviations

ECOPD; exacerbation of COPD; HFNC, high-flow nasal cannula; Pdi, transdiaphragmatic pressure swing; Pdi,sniff, maximal transdiaphragmatic pressure during sniff maneuver; PEEPi,dyn, dynamic intrinsic positive end-expiratory pressure; Pes, esophageal pressure swing; Pnose, nasal pressure swing.

Figure 3. Association between dynamic intrinsic PEEP and respiratory muscle ultrasound indices.

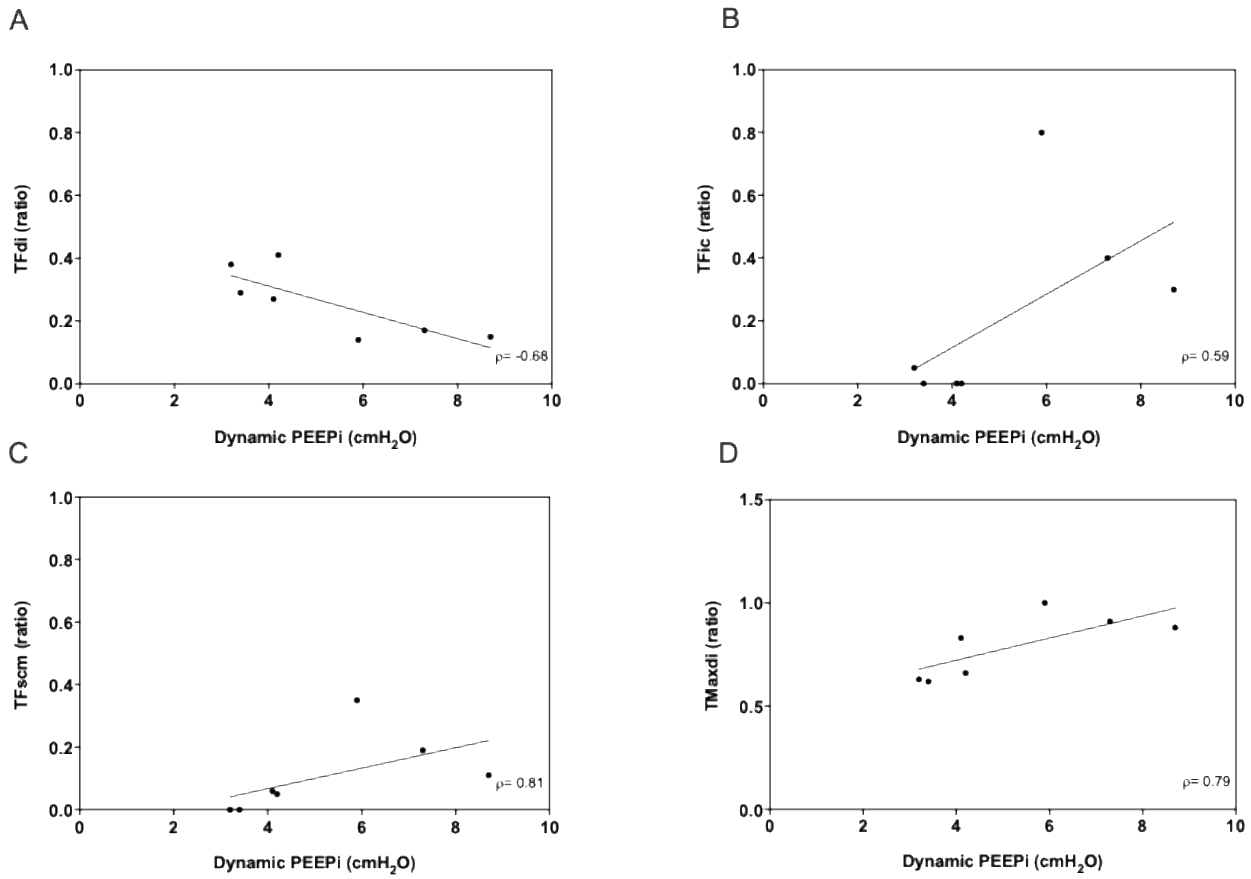

Figure 3. Scatterplots showing the relationship between dynamic intrinsic positive end-expiratory pressure (PEEPi,dyn) and ultrasound-derived indices of inspiratory muscle recruitment. Dynamic PEEPi was inversely correlated with diaphragmatic thickening fraction (TFdi; A) and directly correlated with intercostal thickening fraction (TFic; B), sternocleidomastoid thickening fraction (TFscm; C), and tidal-to-maximal diaphragmatic thickening ratio (TMaxdi; D). Spearman correlation coefficients are reported in each panel. Lines represent linear fit for visual display.

Abbreviations

PEEPi,dyn, dynamic intrinsic positive end-expiratory pressure; TFdi, diaphragmatic thickening fraction; TFic, intercostal thickening fraction; TFscm, sternocleidomastoid thickening fraction; TMaxdi, tidal-to-maximal diaphragmatic thickening ratio.

Figure 4. Association between dynamic intrinsic PEEP, breathing pattern, and dyspnea.

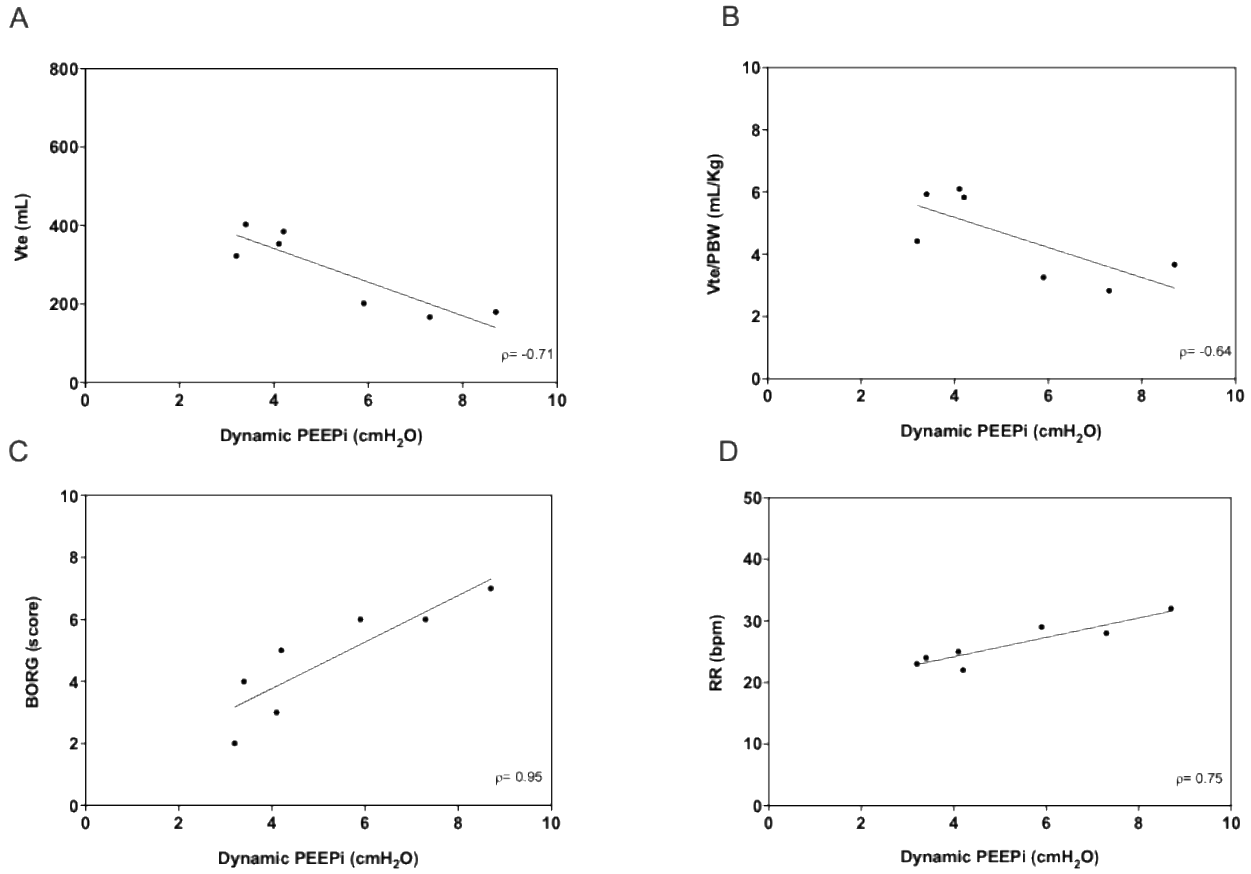

Figure 4. Scatterplots showing the relationship between dynamic intrinsic positive end-expiratory pressure (PEEPi,dyn), breathing pattern, and dyspnea during HFNC treatment. Dynamic PEEPi was inversely correlated with expiratory tidal volume (Vte; A) and Vte normalized to predicted body weight (Vte/PBW; B), and directly correlated with Borg dyspnea score (C) and respiratory rate (RR; D). Spearman correlation coefficients are reported in each panel. Lines represent linear fit for visual display.

Abbreviations

HFNC, high-flow nasal cannula; PBW, predicted body weight; PEEPi,dyn, dynamic intrinsic positive end-expiratory pressure; RR, respiratory rate; Vte, expiratory tidal volume.

3.3 Baseline dynamic PEEPi and T0–T1 physiological changes

Associations between baseline dynamic PEEPi and relative changes in physiological variables from T0 to T1 are shown in the Supplement. For inspiratory effort indices, baseline dynamic PEEPi correlated directly with percentage changes in tidal Pes and Pnose swings, with ρ=0.71 and ρ=0.61, respectively (**Figure 5**, **panel A** and **C**). Conversely, inverse correlations were observed with percentage changes in Pdi and Pdisniff, with ρ=−0.36 and ρ=−0.93, respectively (**Figure 5**, **panel B** and **D**). For respiratory muscle US indices, baseline dynamic PEEPi was inversely correlated with percentage changes in TFdi with ρ=−0.87 (**Figure 6**, **panel A**). Direct correlations were observed with absolute changes in TFic, TFscm and percentage change in TMaxdi with ρ=0.87, ρ=0.82 and ρ=0.67 respectively (**Figure 6**, **panel B, C and D**). Baseline dynamic PEEPi correlated directly with percentage changes in dynamic PEEPi and RR (ρ=0.86 and ρ=0.64, **Figure 7**, panel **A** and **D**, respectively). An inverse correlation was observed with percentage change in Vte/PBW, with ρ=−0.82 (**Figure 7**, **panel B**), whereas no meaningful correlation was found with the percentage change in Borg score (ρ=−0.02; **eFigure 7, panel C**).

Figure 5. Association between baseline dynamic intrinsic PEEP and changes in inspiratory effort during HFNC.

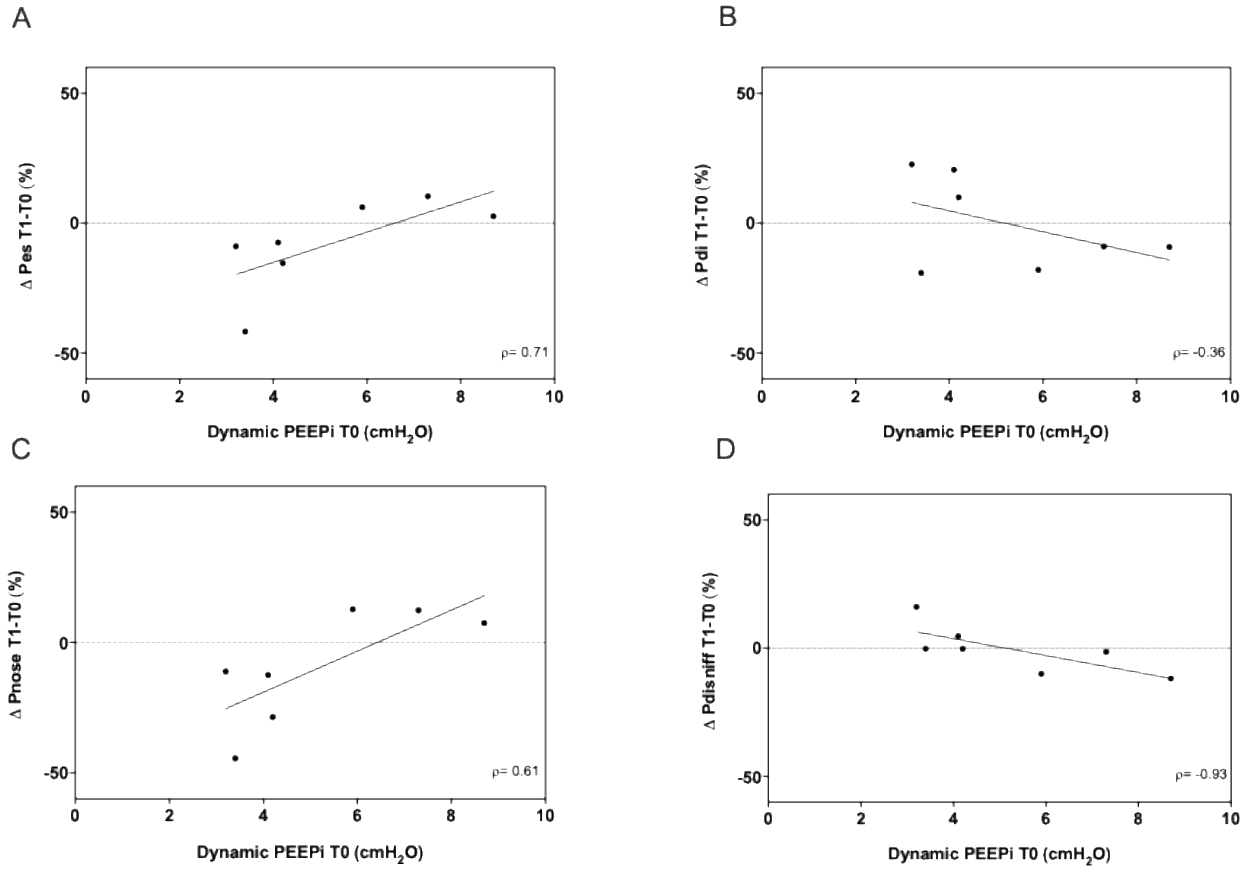

Figure 5. Scatterplots showing the relationship between baseline dynamic intrinsic positive end-expiratory pressure (PEEPi,dyn) and percentage changes in inspiratory effort indices from HFNC initiation (T0) to reassessment after 2 hours of treatment (T1). Baseline PEEPi,dyn was directly correlated with percentage changes in tidal esophageal pressure swing (Pes; A) and tidal nasal pressure swing (Pnose; C), and inversely correlated with percentage changes in transdiaphragmatic pressure swing (Pdi; B) and maximal transdiaphragmatic pressure during sniff maneuver (Pdi,sniff; D). Spearman correlation coefficients are reported in each panel. Lines represent linear fit for visual display.

Abbreviations

HFNC, high-flow nasal cannula; Pdi, transdiaphragmatic pressure swing; Pdi,sniff, maximal transdiaphragmatic pressure during sniff maneuver; PEEPi,dyn, dynamic intrinsic positive end-expiratory pressure; Pes, esophageal pressure swing; Pnose, nasal pressure swing.

Figure 6. Association between baseline dynamic intrinsic PEEP and changes in respiratory muscle ultrasound indices during HFNC.

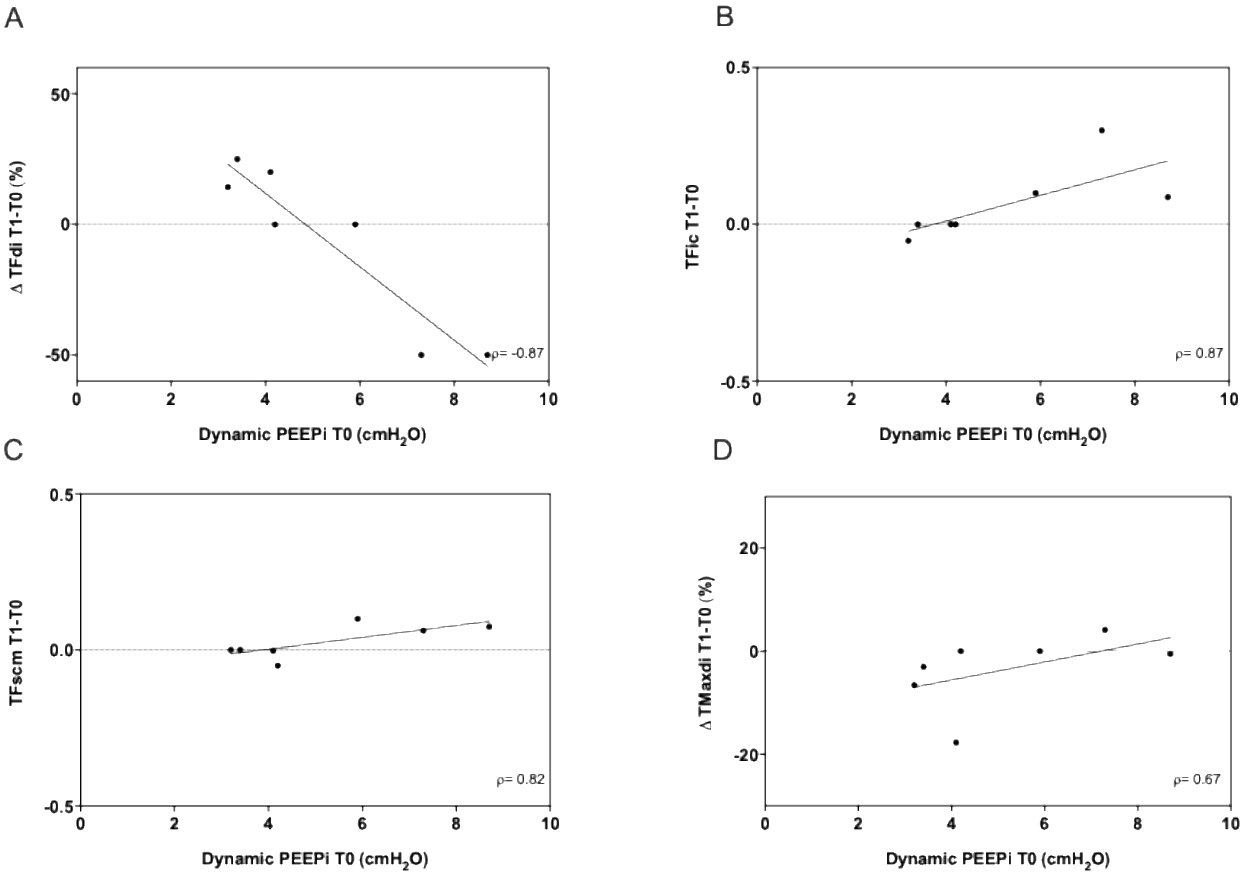

Figure 6. Scatterplots showing the relationship between baseline dynamic intrinsic positive end-expiratory pressure (PEEPi,dyn) and changes in ultrasound-derived indices of inspiratory muscle recruitment from HFNC initiation (T0) to reassessment after 2 hours of treatment (T1). Baseline PEEPi,dyn was inversely correlated with percentage change in diaphragmatic thickening fraction (TFdi; A), and directly correlated with absolute changes in intercostal thickening fraction (TFic; B), sternocleidomastoid thickening fraction (TFscm; C), and percentage change in tidal-to-maximal diaphragmatic thickening ratio (TMaxdi; D). Spearman correlation coefficients are reported in each panel. Lines represent linear fit for visual display.

Abbreviations

PEEPi,dyn, dynamic intrinsic positive end-expiratory pressure; TFdi, diaphragmatic thickening fraction; TFic, intercostal thickening fraction; TFscm, sternocleidomastoid thickening fraction; TMaxdi, tidal-to-maximal diaphragmatic thickening ratio.

Figure 7. Association between baseline dynamic intrinsic PEEP and changes in respiratory mechanics, breathing pattern, and dyspnea during HFNC.

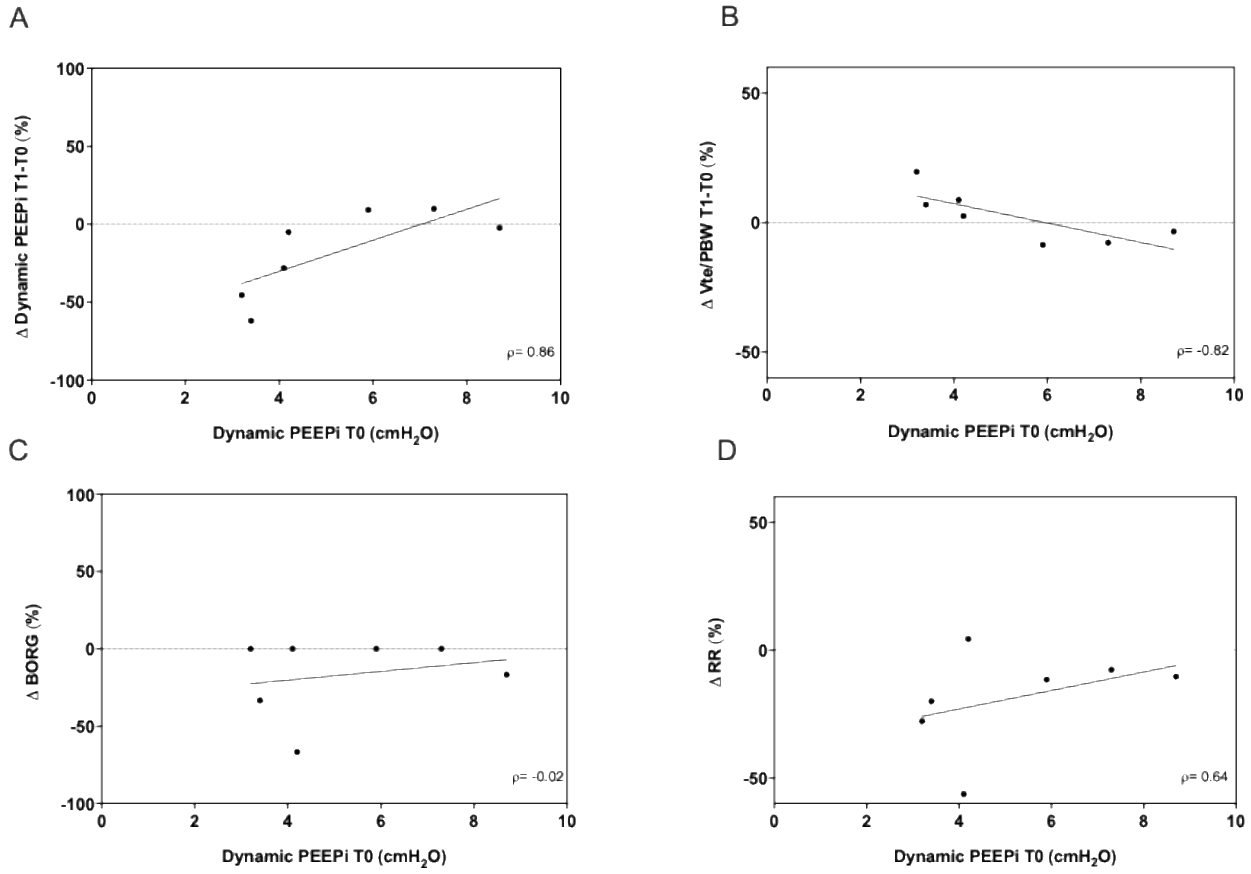

Figure 7. Scatterplots showing the relationship between baseline dynamic intrinsic positive end-expiratory pressure (PEEPi,dyn) and percentage changes in respiratory mechanics, breathing pattern, and dyspnea from HFNC initiation (T0) to reassessment after 2 hours of treatment (T1). Baseline PEEPi,dyn was directly correlated with percentage changes in dynamic PEEPi (A) and respiratory rate (RR; D), and inversely correlated with percentage change in expiratory tidal volume normalized to predicted body weight (Vte/PBW; B). No meaningful correlation was observed with percentage change in Borg dyspnea score (C). Spearman correlation coefficients are reported in each panel. Lines represent linear fit for visual display.

Abbreviations

HFNC, high-flow nasal cannula; PBW, predicted body weight; PEEPi,dyn, dynamic intrinsic positive end-expiratory pressure; RR, respiratory rate; Vte, expiratory tidal volume.

4. DISCUSSION

This prospective physiological proof-of-concept study is the first to systematically explore the relationship between dynamic PEEPi and the physiological response to HFNC in patients with ECOPD. Our data suggest that the magnitude of dynamic hyperinflation may be a key modulator of inspiratory effort, respiratory muscle recruitment, breathing pattern, and dyspnea during HFNC, and that it may influence the trajectory of physiological changes over the first hours of treatment.

The role of HFNC in ECOPD remains a matter of active debate. While NIV is the established standard of care for hypercapnic respiratory failure, recent clinical trials have yielded conflicting results regarding the comparative effectiveness of HFNC[72]. The RENOVATE trial demonstrated noninferiority of HFNC versus NIV for endotracheal intubation or death within 7 days across multiple acute respiratory failure subgroups; however, the COPD exacerbation with respiratory acidosis subgroup included only 77 patients, and a post hoc analysis without dynamic borrowing across patient groups revealed qualitatively different results, underscoring persistent uncertainty[73]. Conversely, Tan et al. found that HFNC failed to meet noninferiority criteria compared with NIV in AECOPD patients with acute-moderate hypercapnic respiratory failure, with a higher treatment failure rate (25.7% vs 14.3%) and a higher intubation rate (14.2% vs 5.4%)[74]. A recent year-in-review concluded that contemporary evidence reinforces NIV as the standard of care for COPD exacerbations, while HFNC may represent a reasonable alternative in selected patients, supporting an individualized, context-specific approach guided by careful monitoring and timely escalation. Critically, however, the physiological determinants of this heterogeneous response remain poorly understood. While HFNC provides dead-space washout, modest positive airway pressure, and improved patient comfort, its capacity to counterbalance the inspiratory threshold load imposed by dynamic hyperinflation — the hallmark mechanical derangement of ECOPD — has never been systematically investigated. This gap is clinically relevant because the degree of dynamic PEEPi may represent a key physiological variable that modulates the response to HFNC and could help identify patients who require early escalation to NIV.

4.1 Dynamic PEEPi and inspiratory threshold loading

In this line, the direct correlations observed between PEEPi,dyn and tidal Pes, Pdi, and Pnose swings are physiologically expected. PEEPi represents the positive elastic recoil pressure of the respiratory system at end-expiration when lung volume exceeds the relaxation volume. Before inspiratory flow can begin, the inspiratory muscles must generate a negative pleural pressure equal in magnitude to PEEPi, an isometric effort that produces no ventilation yet consumes a substantial fraction of the available pressure-generating capacity[75,76] . The total Pes swing therefore reflects not only the pressure needed to overcome respiratory system elastance and resistance during tidal inflation, but also this threshold component, which increases in direct proportion to the degree of dynamic hyperinflation[77]. The

correlation with Pdi indicates that the diaphragm bears a significant share of this excess load. Critically, the inverse correlation between PEEPi,dyn and Pdisniff suggests that patients with greater dynamic hyperinflation may exhibit reduced maximal diaphragmatic pressure-generating capacity. The physiological basis for this is well established: hyperinflation shortens diaphragmatic fiber length, flattens the dome, reduces the zone of apposition, and shifts the muscle to a less favorable portion of its force-length curve[61,78,79]. De Troyer demonstrated that while chronic hyperinflation triggers sarcomere dropout — an adaptive remodeling that partially preserves force generation at the new operating length — the diaphragm's capacity to descend during inspiration remains impaired, and its rib cage expanding action may even become paradoxical in severe hyperinflation[61]. Similowski et al. showed that the diaphragm in stable COPD patients with chronic hyperinflation performs better than predicted from lung volume alone, suggesting partial adaptation, but this compensatory reserve may be overwhelmed during acute exacerbations when PEEPi rises abruptly[78]. The coexistence of an increased threshold load and a reduced maximal force capacity implies that the diaphragm in hyperinflated patients operates at a higher fraction of its maximal capacity during each tidal breath, narrowing the contractile reserve. This interpretation is consistent with the findings that PEEPi,dyn inversely correlates with Pdisniff in ECOPD patients who failed NIV, identifying dynamic hyperinflation as a primary mechanical driver of diaphragmatic dysfunction[80].

4.2 Respiratory muscle redistribution

The respiratory muscle US findings provide a complementary perspective on these pressure-based observations. The inverse correlation between PEEPi,dyn and TFdi, coupled with direct correlations with TFscm and TFic, is consistent with a shift from diaphragm-dominant to accessory muscle-dependent ventilation as the inspiratory threshold load increases. This pattern can be understood through the differential susceptibility of inspiratory muscles to hyperinflation: the diaphragm undergoes the largest length change and geometric distortion, whereas the parasternal intercostals and sternocleidomastoid are less affected because their length changes during hyperinflation are proportionally smaller[63,79]. As the diaphragm loses mechanical advantage, neural drive is redistributed to these extra-diaphragmatic muscles, which can partially compensate by expanding the rib cage through sternal elevation and intercostal space widening — though this strategy is energetically costly and has been associated with greater disease severity[63]. The direct correlation between PEEPi,dyn and TMaxdi — the ratio of tidal to maximal diaphragmatic thickening — provides convergent evidence from an independent modality that the diaphragm in the most hyperinflated patients may be operating near its physiological ceiling during tidal breathing, with minimal reserve to accommodate further increases in ventilatory demand[80,81].

4.3 Ventilatory inefficiency and dyspnoea

The breathing pattern associations are mechanistically coherent with the above findings. The inverse correlation between PEEPi,dyn and tidal volume likely reflects the fact that a greater proportion of the total inspiratory pressure is consumed by the threshold load, leaving less effective pressure for tidal volume generation[75,92]. This is compounded by the increased end-expiratory lung volume itself: at higher lung volumes, the respiratory system operates on a flatter portion of the pressure-volume curve, where greater pressure increments yield smaller volume changes[82]. The compensatory increase in respiratory rate partially preserves minute ventilation but is inherently self-defeating: shorter expiratory times impede lung emptying, perpetuating or worsening air trapping in a positive feedback loop [77,82]. Moreover, higher respiratory rates reduce the end-expiratory pause during which HFNC can wash out upper airway dead space — Pinkham et al. demonstrated that dead-space clearance at 20 L/min dropped from 43 mL at a respiratory rate of 15/min to only 9 mL at 45/min — potentially attenuating one of the principal physiological benefits of HFNC in precisely the patients who need it most[83]. The very strong correlation between PEEPi,dyn and Borg dyspnoea score (ρ=0.95), while striking, should be interpreted cautiously given the small sample size. Nonetheless, it is consistent with the concept of neuromechanical dissociation — the mismatch between elevated inspiratory neural drive and the constrained mechanical output of the respiratory system — which has been identified as a central mechanism of dyspnoea in COPD across the severity spectrum[84,85]. James et al. demonstrated that dyspnoea intensity during exercise is strongly correlated with diaphragm EMG expressed as a percentage of maximum (r=0.73), and that onset of critical inspiratory constraints and neuromechanical dissociation amplifies dyspnoea at progressively lower ventilation with worsening disease severity[86]. Our findings suggest that an analogous mechanism may operate at rest during ECOPD, where the threshold load imposed by PEEPi drives the dissociation between neural drive and ventilatory output.

4.4 Why HFNC may be insufficient in high-PEEPi patients

These observations converge on a central physiological consideration: the level of external PEEP generated by HFNC may be insufficient to counterbalance PEEPi in patients with significant dynamic hyperinflation. At 40 L/min with the mouth open — the typical clinical scenario during HFNC — nasopharyngeal pressure reaches only approximately 0.8 cmH_2O, and even with mouth closure only 6.8 cmH_2O[87]. In clinical practice, Pinkham et al. measured a median PEEP of only 1.71 cmH_2O at 45 L/min in COPD patients with acute respiratory failure[83]. These values are substantially lower than the PEEPi,dyn typically encountered in ECOPD[80,81]. In patients with low PEEPi,dyn, this modest pressure — combined with dead-space washout and improved ventilatory efficiency — may be sufficient to reduce the work of breathing, as demonstrated by Di Mussi et al. in post-extubation COPD

patients[88]. In patients with high PEEPi,dyn, however, the unrelieved threshold load may dominate the physiological picture. This interpretation is consistent with the study by Guan et al., showing that NIV produces more pronounced reductions in inspiratory effort compared with HFNC in hypercapnic respiratory failure, precisely because NIV provides adjustable external PEEP that can be titrated to match PEEPi and pressure support that directly unloads the respiratory muscles[64]. Ranieri et al. demonstrated that in COPD patients with expiratory flow limitation, external PEEP can counterbalance PEEPi without causing further hyperinflation up to a critical threshold, beyond which additional lung distension occurs — a titration that HFNC, with its fixed and low-level pressure output, cannot achieve[75].

4.5 Short-term physiological trajectories

The longitudinal analysis suggests that baseline PEEPi,dyn may also modulate the trajectory of physiological change during HFNC. The direct correlations between baseline PEEPi,dyn and percentage changes in Pes, Pnose, TFic, TFscm, TMaxdi, and respiratory rate — together with inverse correlations with changes in TFdi and Vte/PBW — raise the possibility that patients with higher baseline PEEPi,dyn may exhibit a less favourable physiological trajectory over the first 2 hours. Rather than improving, these patients appear to show increasing inspiratory effort, progressive diaphragmatic disengagement, and intensifying accessory muscle recruitment. The strong direct correlation between baseline PEEPi,dyn and its own percentage change (ρ=0.86) is consistent with a self-reinforcing cycle in which high PEEPi,dyn drives tachypnoea, which shortens expiratory time, which worsens air trapping, which further elevates PEEPi,dyn[82]. The inverse correlations with changes in Pdi and Pdisniff may reflect progressive diaphragmatic fatigue or a ceiling effect in patients whose diaphragm is already maximally loaded, though this interpretation remains speculative given the sample size. The absence of a meaningful correlation with Borg score changes may reflect the multidimensional nature of dyspnoea perception, which integrates not only mechanical load but also chemoreceptive, affective, and cognitive inputs[84], or may simply reflect insufficient statistical power.

4.6 Clinical implications

From a clinical perspective, these findings raise the hypothesis that PEEPi,dyn could serve as a physiological marker to identify ECOPD patients who may not respond adequately to HFNC alone and who might benefit from early escalation to NIV. This concept is consistent with the 2026 GOLD recommendations, which position HFNC as an option for hypoxemic patients, those unable to tolerate NIV, or as a bridge during NIV interruptions, while maintaining NIV as first-line for hypercapnic respiratory failure[89]. The ERS Clinical Practice Guidelines similarly recommend NIV over HFNC in this population[90]. Our data provide a potential physiological rationale for these recommendations by suggesting that HFNC benefits may be attenuated in patients with the greatest dynamic hyperinflation.

4.7 Strengths and limitations

The integration of esophageal manometry, respiratory muscle US, and nasal pressure monitoring represents a methodological strength. The convergent findings across these modalities strengthen internal consistency and support the potential for multimodal bedside phenotyping. The strong correlation between Pnose and Pes swings supports the role of nasal pressure as a non-invasive surrogate for monitoring inspiratory effort during HFNC, extending prior validation in de novo acute respiratory failure to the ECOPD population[50].

Several limitations must be acknowledged. The small sample size (n=7) substantially limits statistical power and precludes multivariable adjustment or definitive conclusions; all correlations should be interpreted as hypothesis-generating. PEEPi,dyn was measured during a brief HFNC interruption rather than during continuous delivery, which may not perfectly reflect conditions during uninterrupted treatment, though the interruption was kept under three minutes to minimize physiological dissipation. The study used a single flow rate (40 L/min); higher flows may generate greater PEEP and enhanced dead-space clearance, potentially modifying the observed relationships[83,91]. The absence of a comparator arm (e.g., NIV or conventional oxygen therapy) limits the ability to attribute physiological patterns specifically to HFNC rather than to the natural course of the exacerbation. Finally, the two-hour observation window may be insufficient to capture the full trajectory of physiological adaptation or deterioration.

5. CONCLUSION

This proof-of-concept study suggests that dynamic PEEPi may be a central modulator of the physiological response to HFNC in ECOPD. Higher PEEPi,dyn was associated with greater inspiratory effort, reduced diaphragmatic function, increased extra-diaphragmatic muscle recruitment, a more constrained breathing pattern, and more severe dyspnea, and these associations appeared to extend to the trajectory of change over the first hours of treatment. These findings provide a physiological framework for understanding the heterogeneity of HFNC response in ECOPD and suggest that bedside assessment of dynamic hyperinflation may help identify patients who require early escalation to NIV. Larger, adequately powered studies are needed to validate these observations and determine whether PEEPi-guided treatment algorithms can improve clinical outcomes.

6. BIBLIOGRAPHY

1. GOLD 2025 Report. Global strategy for the diagnosis, management, and prevention of chronic obstructive pulmonary disease. Augusti A: Global Initiative for Chronic Obstructive Lung Disease; 2024; [accessed 2025 Jan 03]. Available from: https://goldcopd.org/2025-gold-report/.
2. Celli BR, Fabbri LM, Aaron SD et al. An Updated Definition and Severity Classification of Chronic Obstructive Pulmonary Disease Exacerbations: The Rome Proposal. Am J Respir Crit Care Med. 2021; 204(11):1251-1258.
3. Agenas. Programma Nazionale Esiti. [accessed 2025 Jan 03]. Available from: https://pne.agenas.it/home (2024).
4. Prediletto I, Giancotti G, Nava S. COPD Exacerbation: Why It Is Important to Avoid ICU Admission. *Journal of Clinical Medicine*. 2023; 12(10):3369.
5. O'Donnell DE, Parker CM. COPD exacerbations. 3: Pathophysiology. *Thorax*. 2006; 61(4):354-61.
6. Rochwerg B, Brochard L, Elliott MW et al. Official ERS/ATS clinical practice guidelines: Noninvasive ventilation for acute respiratory failure. *Eur Respir J*. 2017; 50(2):1602426.
7. Brochard L, Mancebo J, Wysocki M et al. Noninvasive ventilation for acute exacerbations of chronic obstructive pulmonary disease. *N Engl J Med*. 1995; 333(13):817–22.
8. Oczkowski S, Ergan B, Bos L, Chatwin M et al. ERS clinical practice guidelines: high-flow nasal cannula in acute respiratory failure. *Eur Respir J*. 2022; 59(4):2101574.
9. Calverley PM. Respiratory failure in chronic obstructive pulmonary disease. *Eur Respir J Suppl.* 2003; 47:26s-30s.
10. Abdo WF, Heunks LM. Oxygen-induced hypercapnia in COPD: myths and facts. *Crit Care*. 2012; 16(5):323.
11. Diaz O, Iglesia R, Ferrer M et al. Effects of noninvasive ventilation on pulmonary gas exchange and hemodynamics during acute hypercapnic exacerbations of chronic obstructive pulmonary disease. *Am J Respir Crit Care Med*. 1997; 156(6):1840-5.
12. Pisani L, Astuto M, Prediletto I et al. High flow through nasal cannula in exacerbated COPD patients: a systematic review. *Pulmonology*. 2019; 25(6):348-354.
13. Gayan-Ramirez G, Decramer M. Mechanisms of striated muscle dysfunction during acute exacerbations of COPD. *J Appl Physiol (1985)*. 2013; 114(9):1291-9.
14. Gayan-Ramirez G, Decramer M. The Respiratory Muscles. In: Grippi MA, Elias JA, Fishman JA, Kotloff RM, Pack AI, Senior RM, Siegel MD. eds. Fishman's Pulmonary Diseases and Disorders, Fifth Edition. McGraw-Hill Education; 2015.
15. McKenzie DK, Butler JE, Gandevia SC. Respiratory muscle function and activation in chronic obstructive pulmonary disease. *J Appl Physiol (1985)*. 2009;107(2):621-9.
16. De Troyer A, Wilson TA. Effect of acute inflation on the mechanics of the inspiratory muscles. *J Appl Physiol (1985)*. 2009;107(1):315-23.

17. Marchioni A, Tonelli R, Fantini R et al. Respiratory Mechanics and Diaphragmatic Dysfunction in COPD Patients Who Failed Non-Invasive Mechanical Ventilation. *Int J Chron Obstruct Pulmon Dis*. 2019; 14:2575-2585.
18. Santana PV, Cardenas LZ, Albuquerque ALP et al. Diaphragmatic ultrasound: a review of its methodological aspects and clinical uses. *J Bras Pneumol*. 2020; 46(6): e20200064.
19. Antenora F, Fantini R, Iattoni A et al. Prevalence and outcomes of diaphragmatic dysfunction assessed by ultrasound technology during acute exacerbation of COPD: A pilot study. *Respirology*. 2017; 22(2):338-344.
20. Marchioni A, Castaniere I, Tonelli R et al. Ultrasound-assessed diaphragmatic impairment is a predictor of outcomes in patients with acute exacerbation of chronic obstructive pulmonary disease undergoing noninvasive ventilation. *Crit Care*. 2018; 22(1):109.
21. De Troyer A, Sampson MG. Activation of the parasternal intercostals during breathing efforts in human subjects. *J Appl Physiol Respir Environ Exerc Physiol*. 1982; 52(3):524-9.
22. Yoshida R, Tomita K, Kawamura K et al. Measurement of intercostal muscle thickness with ultrasound imaging during maximal breathing. *J Phys Ther Sci*. 2019; 31(4):340-343.
23. Dres M, Dubé BP, Goligher E et al. Usefulness of Parasternal Intercostal Muscle Ultrasound during Weaning from Mechanical Ventilation. *Anesthesiology.* 2020; 132(5):1114-1125.
24. Wallbridge P, Parry SM, Das S et al. Parasternal intercostal muscle ultrasound in chronic obstructive pulmonary disease correlates with spirometric severity. *Sci Rep*. 2018; 8(1):15274.
25. Umbrello M, Formenti P, Lusardi AC et al. Oesophageal pressure and respiratory muscle ultrasonographic measurements indicate inspiratory effort during pressure support ventilation. *Br J Anaesth*. 2020; 125(1): e148-e157.
26. Formenti P, Umbrello M, Dres M et al. Ultrasonographic assessment of parasternal intercostal muscles during mechanical ventilation. *Ann Intensive Care*. 2020; 10(1):120.
27. Gandevia SC, Leeper JB, McKenzie DK et al. Discharge frequencies of parasternal intercostal and scalene motor units during breathing in normal and COPD subjects. *Am J Respir Crit Care Med*. 1996; 153(2):622-8.
28. De Troyer A, Estenne M. Coordination between rib cage muscles and diaphragm during quiet breathing in humans. *J Appl Physiol Respir Environ Exerc Physiol*. 1984; 57((3)):899–906.
29. Shiraishi M, Higashimoto Y, Sugiya R et al. Sternocleidomastoid Muscle Thickness Correlates with Exercise Tolerance in Patients with COPD. *Respiration*. 2023; 102(1):64-73.
30. Magdy, D. · Metwally, A. The utility of HACOR score in predicting failure of high-flow nasal oxygen in acute hypoxemic Respiratory failure Adv Respir Med. 2021; 89(1):23-29 – 15 Duan, J. · Yang, J. · Jiang, L. Prediction of noninvasive ventilation failure using the ROX index in patients with de novo acute respiratory failure Ann Intensive Care. 2022; 12(1):110.

31. Carteaux, G. · Parfait, M. · Combet, M. ... Patient self-inflicted lung injury: a practical review, J Clin Med. 2021; 10(12):2738.
32. Tonelli, R. · Fantini, R. · Bruzzi, G. ..., Effect of high flow nasal oxygen on inspiratory effort of patients with acute hypoxic respiratory failure and do not intubate orders, Intern Emerg Med. 2024; 19(2):333-342.
33. Akoumianaki, E. · Maggiore, S.M. · Valenza, F. ..., The application of esophageal pressure measurement in patients with Respiratory failure, Am J Respir Crit Care Med. 2014; 189(5):520-531.
34. Tonelli, R. · Fantini, R. · Tabbì, L. ..., Early inspiratory effort assessment by esophageal manometry predicts noninvasive ventilation outcome in de novo respiratory failure. A pilot study, Am J Respir Crit Care Med. 2020; 202(4):558-567]
35. Mojoli, F. · Iotti, G.A. · Torriglia, F. ..., In vivo calibration of esophageal pressure in the mechanically ventilated patient makes measurements reliable, Crit Care. 2016; 20(1):98.
36. Milic-Emili J, Mead J, Turner JM, Glauser EM. Mechanics of breathing: distribution of pleural pressure in man. J Appl Physiol. 1964.
37. Baydur A, Behrakis PK, Zin WA, Jaeger M, Milic-Emili J. A simple method for assessing the validity of the esophageal balloon technique. Am Rev Respir Dis. 1982.
38. Akoumianaki E, Maggiore SM, Valenza F, et al. The application of esophageal pressure measurement in patients with respiratory failure. Intensive Care Med. 2014.
39. D'Angelo E, Prandi E. Esophageal pressure and pleural pressure: limitations and physiological considerations. Respir Physiol Neurobiol. 2004.
40. Loring SH, Topulos GP, Hubmayr RD. Transpulmonary pressure: the importance of the chest wall. Am J Respir Crit Care Med. 2016.
41. Talmor D, Sarge T, Malhotra A, et al. Mechanical ventilation guided by esophageal pressure in acute lung injury. N Engl J Med. 2008.
42. Norman RG, Goldstein CA, et al. Detection of respiratory effort and airflow limitation using nasal pressure. Sleep. 1997.
43. Ayappa I, Rapoport DM. The nasal pressure technique: principles and clinical applications. Am J Respir Crit Care Med. 2003.
44. Berry RB, Budhiraja R, Gottlieb DJ, et al. Rules for scoring respiratory events in sleep: update of the AASM manual. Sleep. 2012.
45. De Troyer A, Estenne M. Functional anatomy of the respiratory muscles. Clin Chest Med. 1988.
46. Goligher EC, Brochard LJ, Reid WD, et al. Diaphragmatic myotrauma and monitoring of respiratory effort during mechanical ventilation. Intensive Care Med. 2018.

47. Demoule A, Hill N, Navalesi P. Can we prevent intubation in patients with ARDS? Intensive Care Med. 2016; 42(5):768-771.
48. Mocellin A, Guidotti F, Rizzato S et al. Monitoring and modulation of respiratory drive in patients with acute hypoxemic respiratory failure in spontaneous breathing. Intern Emerg Med. 2024; 19(8):2105-2119.
49. Yoshida T, Grieco DL, Brochard L. Guiding ventilation with transpulmonary pressure. Intensive Care Med. 2019; 45(4):535-538.
50. Tonelli R, Cortegiani A, Marchioni A et al. Nasal pressure swings as the measure of inspiratory effort in spontaneously breathing patients with de novo acute respiratory failure. Crit Care. 2022; 26(1):70.
51. Tobin MJ. Principles and Practice of Mechanical Ventilation. McGraw-Hill.
52. West JB. Respiratory Physiology: The Essentials. Lippincott Williams & Wilkins.
53. Slutsky AS, Ranieri VM. Ventilator-induced lung injury. N Engl J Med. 2013; 369:2126–2136.
54. Brochard L, Mancebo J, Wysocki M, et al. Noninvasive ventilation for COPD exacerbations. N Engl J Med. 1995.
55. Tuxen DV, Lane S. The effects of ventilatory pattern on hyperinflation in severe COPD. Am Rev Respir Dis. 1987.
56. Rossi A, Polese G, Brandi G, et al. Intrinsic positive end-expiratory pressure (PEEPi). Eur Respir J. 1995.
57. Laghi F, Tobin MJ. Disorders of the respiratory muscles in COPD. Am J Respir Crit Care Med. 2003.
58. Gattinoni L, Tonetti T, Quintel M. Respiratory mechanics in ARDS and PEEP titration. Intensive Care Med. 2017.
59. Liu L, Xia F, Yang Y, et al. Neural versus pneumatic control of pressure support in patients with chronic obstructive pulmonary diseases at different levels of positive end expiratory pressure: a physiological study. Crit Care. 2015;19(1):244. doi:10.1186/s13054-015-0971-0
60. Goldberg P, Reissmann H, Maltais F, Ranieri M, Gottfried S. Efficacy of noninvasive CPAP in COPD with acute respiratory failure. Eur Respir J. 1995;8(11):1894-1900. doi:10.1183/09031936.95.08111894
61. De Troyer A. Effect of hyperinflation on the diaphragm. Eur Respir J. 1997;10(3):708-713. doi:10.1183/09031936.97.10030708
62. López-Rey JM, Beyer B, García-Vargas E, Torres-Sánchez I, García-Río F, Bastir M. Three-dimensional geometric morphometric analysis of diaphragmatic dome motion in COPD patients. Anat Rec. Published online February 11, 2026: ar.70161. doi:10.1002/ar.70161
63. Tabbì L, Marchioni A, Messina J, et al. Ultrasound-based evaluation of inspiratory muscle effort in patients with type 2 respiratory failure secondary to exacerbation of chronic obstructive pulmonary disease. Eur J Intern Med. Published online December 2025:106649. doi: 10.1016/j.ejim.2025.106649
64. Guan L, Xu J, He Z, et al. Efficiency of neural respiratory drive changes during non-invasive ventilation and high-flow nasal cannula oxygen therapy in AECOPD patients with acute hypercapnic respiratory failure: A randomised cross-over study. Ann Intensive Care. 2026; 16:100019. doi: 10.1016/j.aicoj.2025.100019

65. Plant PK, Owen JL, Elliott MW. Early use of non-invasive ventilation in acute exacerbations of COPD. Lancet. 2000.
66. Nava S, Hill N. Non-invasive ventilation in acute respiratory failure. Lancet. 2009.
67. Frat JP, Thille AW, Mercat A, et al. High-flow oxygen through nasal cannula in acute hypoxemic respiratory failure. N Engl J Med. 2015.
68. Nishimura M. High-flow nasal cannula oxygen therapy in adults. J Intensive Care. 2015.
69. Roca O, Riera J, Torres F, Masclans JR. High-flow oxygen therapy in acute respiratory failure. Respir Care. 2010–2012 literature series.
70. Pisani L, et al. High-flow nasal cannula in COPD: physiological effects and clinical applications. Intensive Care Med. 2017–2020 reviews.
71. Bräunlich J, Wirtz H. Nasal high-flow in COPD and hypercapnia: physiological rationale. Respir Med. 2018
72. Cortegiani A, Crimi C, Noto A, et al. Effect of high-flow nasal therapy on dyspnea, comfort, and respiratory rate. Crit Care. 2019;23(1):201. doi:10.1186/s13054-019-2473-y
73. RENOVATE Investigators and the BRICNet Authors, Francio F, Weigert RM, et al. High-Flow Nasal Oxygen vs Noninvasive Ventilation in Patients With Acute Respiratory Failure: The RENOVATE Randomized Clinical Trial. JAMA. 2025;333(10):875. doi:10.1001/jama.2024.26244
74. Tan D, Wang B, Cao P, et al. High flow nasal cannula oxygen therapy versus non-invasive ventilation for acute exacerbations of chronic obstructive pulmonary disease with acute-moderate hypercapnic respiratory failure: a randomized controlled non-inferiority trial. Crit Care. 2024;28(1):250. doi:10.1186/s13054-024-05040-9
75. Ranieri V, Dambrosio M, Brienza N. Intrinsic PEEP and cardiopulmonary interaction in patients with COPD and acute ventilatory failure. Eur Respir J. 1996;9(6):1283-1292. doi:10.1183/09031936.96.09061283
76. Parrilla F, Morán I, Roche-Campo F, Mancebo J. Ventilatory Strategies in Obstructive Lung Disease. Semin Respir Crit Care Med. 2014;35(04):431-440. doi:10.1055/s-0034-1382155
77. Tonelli R, Michelacci S, Verduri A, Clini E. Physiopathology of Exacerbation of Chronic Obstructive Pulmonary Disease. Semin Respir Crit Care Med. Published online February 12, 2026: a-2811-3019. doi:10.1055/a-2811-3019
78. Similowski T, Yan S, Gauthier AP, Macklem PT, Bellemare F. Contractile Properties of the Human Diaphragm during Chronic Hyperinflation. N Engl J Med. 1991;325(13):917-923. doi:10.1056/NEJM199109263251304
79. Decramer M. Hyperinflation and respiratory muscle interaction. Eur Respir J. 1997;10(4):934-941. doi:10.1183/09031936.97.10040934
80. Vitacca M, Ceriana P, Prediletto I, et al. Intrinsic Dynamic Positive End-Expiratory Pressure in Stable Patients with Chronic Obstructive Pulmonary Disease. Respiration. 2020;99(12):1129-1135. doi:10.1159/000511266

81. Ceriana P, Vitacca M, Carlucci A, Paneroni M, Pisani L, Nava S. Changes of Respiratory Mechanics in COPD Patients from Stable State to Acute Exacerbations with Respiratory Failure. COPD J Chronic Obstr Pulm Dis. 2017;14(2):150-155. doi:10.1080/15412555.2016.1254173
82. D'Cruz RF, Wilkins D, Jolley CJ. Exercise-induced dynamic hyperinflation in chronic obstructive pulmonary disease. Exp Physiol. 2026;111(5):2476-2484. doi:10.1113/EP091459
83. Pinkham M, Tatkov S. Effect of flow and cannula size on generated pressure during nasal high flow. Crit Care. 2020;24(1):248. doi:10.1186/s13054-020-02980-w
84. O'Donnell DE. COPD exacerbations {middle dot} 3: Pathophysiology. Thorax. 2006;61(4):354-361. doi:10.1136/thx.2005.041830
85. Jolley CJ, Luo YM, Steier J, Rafferty GF, Polkey MI, Moxham J. Neural respiratory drive and breathlessness in COPD. Eur Respir J. 2015;45(2):355-364. doi:10.1183/09031936.00063014
86. James MD, Phillips DB, Vincent SG, et al. Exertional dyspnoea in patients with mild-to-severe chronic obstructive pulmonary disease: neuromechanical mechanisms. J Physiol. 2022;600(18):4227-4245. doi:10.1113/JP283252
87. Vieira F, Bezerra FS, Coudroy R, et al. High-flow nasal cannula compared with continuous positive airway pressure: a bench and physiological study. J Appl Physiol. 2022;132(6):1580-1590. doi:10.1152/japplphysiol.00416.2021
88. Di Mussi R, Spadaro S, Stripoli T, et al. High-flow nasal cannula oxygen therapy decreases postextubation neuroventilatory drive and work of breathing in patients with chronic obstructive pulmonary disease. Crit Care. 2018;22(1):180. doi:10.1186/s13054-018-2107-9
89. Global Initiative for Chronic Obstructive Lung Disease. Global Strategy for the Diagnosis, Management, and Prevention of Chronic Obstructive Pulmonary Disease: 2026 Report. Global Initiative for Chronic Obstructive Lung Disease. https://goldcopd.org/2026-gold-report-and-pocket-guide/
90. Rochwerg B, Brochard L, Elliott MW, et al. Official ERS/ATS clinical practice guidelines: noninvasive ventilation for acute respiratory failure. Eur Respir J. 2017;50(2):1602426. doi:10.1183/13993003.02426-2016
91. Mauri T, Turrini C, Eronia N, et al. Physiologic Effects of High-Flow Nasal Cannula in Acute Hypoxemic Respiratory Failure. Am J Respir Crit Care Med. 2017;195(9):1207-1215. doi:10.1164/rccm.201605-0916OC
92. Nava S, Bruschi C, Rubini F, Palo A, Iotti G, Braschi A. Respiratory response and inspiratory effort during pressure support ventilation in COPD patients. Intensive Care Med. 1995;21(11):871-879. doi:10.1007/BF01712327